Nested smoothing algorithms for inference and tracking of heterogeneous multi-scale state-space systems

Sara Pérez-Vieites, Harold Molina-Bulla, Joaquín Míguez

Department of Signal Theory & Communications, Universidad Carlos III de Madrid.
Avenida de la Universidad 30, 28911 Leganés, Madrid, Spain.

Abstract

Multi-scale problems, where variables of interest evolve in different time-scales and live in different state-spaces. can be found in many fields of science. Here, we introduce a new recursive methodology for Bayesian inference that aims at estimating the static parameters and tracking the dynamic variables of these kind of systems. Although the proposed approach works in rather general multi-scale systems, for clarity we analyze the case of a heterogeneous multi-scale model with 3 time-scales (static parameters, slow dynamic state variables and fast dynamic state variables). The proposed scheme, based on nested filtering methodology of [26], combines three intertwined layers of filtering techniques that approximate recursively the joint posterior probability distribution of the parameters and both sets of dynamic state variables given a sequence of partial and noisy observations. We explore the use of sequential Monte Carlo schemes in the first and second layers while we use an unscented Kalman filter to obtain a Gaussian approximation of the posterior probability distribution of the fast variables in the third layer. Some numerical results are presented for a stochastic two-scale Lorenz 96 model with unknown parameters.

Keywords: filtering; Kalman; Monte Carlo; Bayesian inference, parameter estimation.

Email addresses: `saperezv@pa.uc3m.es` (Sara Pérez-Vieites), `hmolina@tsc.uc3m.es` (Harold Molina-Bulla), `joaquin.miguez@uc3m.es` (Joaquín Míguez)

1. Introduction

Multi-scale problems can be found naturally in many fields of science, such as biology, chemistry, fluid dynamics and material science, where processes at different time and/or spatial scales may be described by diverse laws [33, 34, 23]. Thanks to the improvements in computational power and the need for ever more faithful models of real-world complex systems, the interest in multi-scale modelling techniques has increased in recent years.

Multi-scale models are aimed at providing an efficient and more accurate representation of a complex system by coupling (sub)models that address different features/attributes at different levels of detail. However, the modeling of such systems is far from straightforward, not only because they are made up of dynamical systems of different characteristics, but also because of often intricate cross dependencies among the relevant physical processes at work [33]. As a consequence, the problem of tracking the evolution of a multi-scale dynamical system involves the prediction and estimation of several sets of variables that live in different state-spaces and evolve in different time scales. Moreover, the tracking of the variables of interest usually has to be performed from the observation of partial and noisy observations. Efficient recursive algorithms for this task are badly needed.

The simplest case of a multi-scale problem consists of a system with unknown static parameters and dynamic state variables, since the parameters may be considered as state variables that evolve at a greater time scale. Hence, it is a multi-scale problem with only two time scales. In general, carrying out both parameter estimation and state tracking at once implies several practical and theoretical difficulties. Within this framework, a few well-principled methods have been proposed in the last few years, though. Two examples of schemes that yield theoretically-guaranteed solutions to this problem are sequential Monte Carlo square (SMC^2) [7] or particle Markov chain Monte Carlo (PMCMC) [3]. They aim at computing the joint posterior probability distribution of all the unknown variables and parameters of the system, which provides all the

information to obtain both point estimates and quantifications of the estimation error. Unfortunately, both SMC^2 and PMCMC are batch techniques. In other words, every time a new observation arrives, the whole sequence of observations may have to to be re-processed from scratch in order to update the estimates, leading to a quadratic increase of the computational effort over time. As an alternative, nested particle filters (NPFs) [8] apply the same principles as SMC^2 in a recursive way. An NPF estimates both parameters and states using a scheme of two intertwined layers of Monte Carlo methods, one inside the other, where the first layer estimates the parameters while the second layer tracks the state dynamical variables. This methodology is better suited for long sequences of observations, however, the use of Monte Carlo in both layers of filters still makes its computational cost prohibitive in high-dimensional problems. Nested hybrid filters (NHFs) [26] are extensions of the NPF that introduce Gaussian filtering techniques in the second layer of the algorithm, reducing the computational cost considerably and making the methodology more appealing for online processing.

In the last few years, other algorithms with nested, or layered, structures (in the vein of SMC^2, NPF or NHF) have been proposed in ordert to address inference in high-dimensional, complex models. The most recent examples are the space-time particle filter (ST-PF) [5] and the nested sequential Monte Carlo (NSMC) [22]. Both methods are intended to outperform classical sequential Monte Carlo (SMC) in high dimensional systems. They rely on spatial structures within the state space (a Markov random field in [22] and an auto-regressive structure in [5]) and, therefore, they may be useful to tackle multiple spatial scales.

One of the most typical examples of multi-scale systems is the two-scale Lorenz 96 model [18, 6, 4]. This is a simplified weather model which includes different spatial and temporal scales. Specifically, it is a heterogeneous multi-scale model, i.e. a model where the macro-scale level description needs to be completed by the data extracted from a micro-scale level [30]. The coupling of both scales can be handled in two different ways:

- applying parameterization [4, 23, 32] or

- using a macro-micro solver [34, 35].

The former is a method used to replace the contribution of the micro-scale level of the model by a simplified process that depends only on the slow state variables of the macro scale. Once the model is simplified to a single scale, many other algorithms can be used to estimate the evolution of the macro-scale process, that is usually the scale of interest. However, the latter method aims at estimating both scales and avoids any simplification of the model. Inference in the two-scale Lorenz 96 model has been addressed using algorithms such as particles filters [36, 21, 16], Gaussian filters [28, 29, 24, 13] or a combination of different methods [14, 27].

In this paper, we propose a generalization of the nested hybrid filter (NHF) methodology aimed at performing recursive Bayesian inference for a class of heterogeneous multi-scale state-space models [1] that can be numerically approximated with a micro-macro solver.We analyse the case of a Lorenz 96 system that displays three time scales (static parameters, slow dynamic state variables at the macro-scale and fast dynamic state variables at the micro-scale), but the methodology works in the same way for more general examples (namely, systems with n scales either in time or space).

The new scheme can be described as a three-layer nested smoother that approximates, in a recursive manner, the posterior probability distributions of the parameters and the two sets of state variables given the sequence of available observations. Specifically, we approximate the posterior probability distribution of the parameters in a first layer of computation, the posterior probability distribution of the slow state variables in a second layer, and the posterior probability distribution of the fast state variables in a third layer. The computations on the second layer are conditional on the candidate parameter values generated on the first layer, while the calculations on the third layer are conditional on the candidates drawn at the first and second layers. The inference techniques used in each layer can vary, leading to different computational costs

4

and degrees of accuracy. As examples that illustrate the methodology, we propose two methods. The first one uses SMC algorithms in the first and second layers, intertwined with an unscented Kalman filter (UKF) [25] in the third layer. Similarly, the second method uses a sequential Monte Carlo (SMC) algorithm in the first layer, but incorporates the use of ensemble Kalman filters (EnKFs) [12] and a extended Kalman filters (EKFs) in the second and third layers of the scheme, respectively.

The rest of the paper is organized as follows. We state the problem to be addressed in Section 2. In Section 3, we describe the optimal smoother for multi-scale systems with static parameters and two sets of dynamic state variables. Two specific methods derived from the general methodology are shown in Section 4. Numerical results for the stochastic two-scale Lorenz 96 model are shown in Section 5 and conclusions are drawn in Section 6.

2. Problem Statement

2.1. State space models

In this chapter we place our attention on state space models that result from the analysis of physical systems that display (intertwined) dynamical features at different time scales. To be specific, let us consider the class of multidimensional stochastic differential equations (SDEs) that can be written as

$$dx = f_x(x, \theta)d\tau + g_x(z, \theta)d\tau + Q_x dv, \tag{1}$$

$$dz = f_z(x, \theta)d\tau + g_z(z, \theta)d\tau + Q_z dw, \tag{2}$$

where

- τ denotes continuous time,

- $x(\tau) \in \mathbb{R}^{d_x}$ and $z(\tau) \in \mathbb{R}^{d_z}$ are the slow and fast states of the system, respectively,

- $f_x \colon \mathbb{R}^{d_x} \times \mathbb{R}^{d_\theta} \to \mathbb{R}^{d_x}$, $g_x \colon \mathbb{R}^{d_z} \times \mathbb{R}^{d_\theta} \to \mathbb{R}^{d_x}$, $f_z \colon \mathbb{R}^{d_x} \times \mathbb{R}^{d_\theta} \to \mathbb{R}^{d_z}$ and $g_z \colon \mathbb{R}^{d_z} \times \mathbb{R}^{d_\theta} \to \mathbb{R}^{d_z}$ are (possibly nonlinear) transition functions parameterized by a fixed vector of unknown parameters, $\theta \in \mathbb{R}^{d_\theta}$,

- Q_x and Q_z are known scaling matrices that control the intensity and covariance of the stochastic perturbations,

- and $v(\tau)$ and $w(\tau)$ are vectors of independent standard Wiener processes with dimension d_x and d_z, respectively.

Equations (1)–(2) do not have closed form solutions for general nonlinear functions f_x, f_z, g_x and g_z and they have to be discretized for their numerical integration. In order to handle the slow and fast time scales, we apply a macro-micro solver [31, 35] that runs an Euler-Maruyama scheme for each set of state variables, albeit with different integration steps. To be specific, we use Δ_z as the integration step of z while $\Delta_x \gg \Delta_z$ is the integration step of x. Then, we can simulate x and z using the pair of difference equations

$$x_t = x_{t-1} + \Delta_x (f_x(x_{t-1}, \theta) + g_x(\bar{z}_t, \theta)) + \sqrt{\Delta_x} Q_x v_t, \tag{3}$$

$$z_n = z_{n-1} + \Delta_z (f_z(x_{\lfloor \frac{n-1}{h} \rfloor}, \theta) + g_z(z_{n-1}, \theta)) + \sqrt{\Delta_z} Q_z w_n, \tag{4}$$

where $x_t \approx x(t\Delta_x)$ and $z_n \approx z(n\Delta_z)$ are the state signals, $t \in \mathbb{N}$ denotes discrete time in the time scale of the slow variables, $n \in \mathbb{N}$ denotes discrete time in the fast time scale, $h = \frac{\Delta_x}{\Delta_z} \in \mathbb{Z}^+$ is the number of fast steps (in the scale of z) per

slow step (in the scale of $\boldsymbol{x}$), $\boldsymbol{v}_t$ and $\boldsymbol{w}_n$ are Gaussian random variables (r.v.s) of zero mean and covariance matrices $\boldsymbol{I}_{d_x}$ and $\boldsymbol{I}_{d_z}$ respectively, and $\bar{\boldsymbol{z}}_t$ is an average of the fast signal computed as

$$\bar{\boldsymbol{z}}_t = \frac{1}{h} \sum_{i=h(t-1)+1}^{ht} \boldsymbol{z}_i. \tag{5}$$

We assume that the available observations may be directly related to both sets of state variables $\boldsymbol{x}_t$ and $\boldsymbol{z}_n$, but only in the (slow) time scale of $\boldsymbol{x}$. To be specific, the t-th observation is a d_y-dimensional r.v., $\boldsymbol{y}_t \in \mathbb{R}^{d_y}$, which we model as

$$\boldsymbol{y}_t = l(\boldsymbol{z}_{ht}, \boldsymbol{x}_t, \boldsymbol{\theta}) + \boldsymbol{r}_t, \tag{6}$$

where $l \colon \mathbb{R}^{d_z} \times \mathbb{R}^{d_x} \times \mathbb{R}^{d_\theta} \to \mathbb{R}^{d_y}$ is a transformation that maps the states into the observation space, and $\boldsymbol{r}_t$ is a zero-mean observational-noise vector with covariance matrix $\boldsymbol{R}$.

2.2. Model inference

We aim at performing *joint* Bayesian estimation of the parameters, $\boldsymbol{\theta}$, and all states, $\boldsymbol{x}$ and $\boldsymbol{z}$, for the state-space model described by Eqs. (3)-(4) and (6). Typically, the three vectors of unknowns are tightly coupled. The estimation of the fixed parameters is necessary to track both sets of state variables and, at the same time, tracking the slow state variables is needed for predicting the time evolution of the fast states and vice versa.

While in many practical applications one is typically interested in filtering, i.e., the computation of the posterior probability density function (pdf) of $\boldsymbol{\theta}$, $\boldsymbol{x}_t$ and $\boldsymbol{z}_n$ (for $n = ht$) given the data sequence $\boldsymbol{y}_{1:t} = \{\boldsymbol{y}_1, \boldsymbol{y}_2, \dots, \boldsymbol{y}_t\}$, we find more convenient to tackle the smoothing pdf $p(\boldsymbol{z}_{h(t-1)+1:ht}, \boldsymbol{x}_{0:t}, \boldsymbol{\theta}|\boldsymbol{y}_{1:t})$. Using the chain rule, we can factorize the latter density as

$$p(\boldsymbol{z}_{h(t-1)+1:ht}, \boldsymbol{x}_{0:t}, \boldsymbol{\theta}|\boldsymbol{y}_{1:t}) = p(\boldsymbol{z}_{h(t-1)+1:ht}|\boldsymbol{x}_{0:t}, \boldsymbol{y}_{1:t}, \boldsymbol{\theta})p(\boldsymbol{x}_{0:t}|\boldsymbol{y}_{1:t}, \boldsymbol{\theta})p(\boldsymbol{\theta}|\boldsymbol{y}_{1:t}), \tag{7}$$

where we identify the three key conditional distributions that we seek to compute (or approximate). Each one of these pdfs can be handled in a different *layer*

7

of computation. Hence, we aim at designing a nested inference algorithm (in the vein of [26]) with three layers. In the first layer we compute $p(\boldsymbol{\theta}|\boldsymbol{y}_{1:t})$, in the second one we obtain $p(\boldsymbol{x}_{0:t}|\boldsymbol{y}_{1:t}, \boldsymbol{\theta})$, and in the third layer we tackle $p(\boldsymbol{z}_{h(t-1)+1:ht}|\boldsymbol{x}_{0:t}, \boldsymbol{y}_{1:t}, \boldsymbol{\theta})$.

Hereafter we describe the methodology for the optimal (yet impractical) calculation of the posterior pdf in Eq. (7) as well as two approximate numerical solutions that admit feasible computational implementations.

2.3. Notation

We use lower-case, regular-face letters, e.g., x, to denote scalar quantities and bold-face, e.g., $\boldsymbol{x}$, to denote vectors. Matrices are represented by bold-face upper-case letters, e.g., $\boldsymbol{X}$. We make no notational difference between between deterministic quantities and random variables (r.v.'s).

If $\boldsymbol{x}$ is a d-dimensional random vector on $\mathbb{R}^d$, we denote its pdf with respect to the Lebesgue measure as $p(\boldsymbol{x})$. This is an argument-wise notation, i.e., if $\boldsymbol{x}$ and $\boldsymbol{y}$ are random vectors, we denote their pdf's as $p(\boldsymbol{x})$ and $p(\boldsymbol{y})$ even if they are possibly different functions (when $\boldsymbol{x}$ and $\boldsymbol{y}$ obey different probability laws). Similary, $p(\boldsymbol{x}, \boldsymbol{y})$ denotes the joint pdf of $\boldsymbol{x}$ and $\boldsymbol{y}$, while $p(\boldsymbol{x}, \boldsymbol{y})$ is the conditional pdf of $\boldsymbol{x}$ given $\boldsymbol{y}$. This notation, which has been broadly used in the field if particle filtering [17, 10, 9, 11], is simple yet sufficient to describe the methodologies in this paper.

We also resort to a more specific notation for Gaussian pdf's. If $\boldsymbol{x}$ is a d-dimensional Gaussian random vector with mean $\bar{\boldsymbol{x}}$ and covariance matrix $\boldsymbol{C} > 0$ then we can explicitly write the pdf $p(\boldsymbol{x})$ as

$$\mathcal{N}(\boldsymbol{x}|\bar{\boldsymbol{x}}, \boldsymbol{C}) = \frac{1}{(2\pi)^{\frac{d}{2}} |\boldsymbol{C}|^{\frac{1}{2}}} \exp\left\{-\frac{1}{2}(\boldsymbol{x} - \bar{\boldsymbol{x}})^\top \boldsymbol{C}^{-1}(\boldsymbol{x} - \bar{\boldsymbol{x}})\right\},$$

where the superscript $^\top$ indicates transposition and $|\boldsymbol{C}|$ denotes the determinant of matrix $\boldsymbol{C}$.

3. Optimal nested smoother

We introduce the optimal nested smoothing algorithm, consisting of three layers, that computes each of the pdfs in Eq. (7). The scheme is summarized in Fig. 1. As a result, we obtain the posterior smoothing density $p(\boldsymbol{z}_{h(t-1)+1:ht}, \boldsymbol{x}_{0:t}, \boldsymbol{\theta}|\boldsymbol{y}_{1:t})$ which, in turn, can be used to compute the optimal filtering pdf, $p(\boldsymbol{z}_{ht}, \boldsymbol{x}_t, \boldsymbol{\theta}|\boldsymbol{y}_{1:t})$, by marginalization if necessary. When the exact computations demanded by this algorithm are not feasible (for general nonlinear and/or non-Gaussian dynamical systems) it serves as a template for approximate numerical schemes, as shown in Section 4.

3.1. First layer: static parameters

The aim of this layer is to compute the posterior pdf of the parameters, $p(\boldsymbol{\theta}|\boldsymbol{y}_{1:t})$, recursively. We assume that the *a priori* density $p(\boldsymbol{\theta})$ is known.

At time t, assume that $p(\boldsymbol{\theta}|\boldsymbol{y}_{1:t-1})$ has been calculated. When a new observation, $\boldsymbol{y}_t$, is obtained, we need to compute the likelihood $p(\boldsymbol{y}_t|\boldsymbol{y}_{1:t-1}, \boldsymbol{\theta})$ in order to obtain the posterior pdf of $\boldsymbol{\theta}$ at time t as

$$p(\boldsymbol{\theta}|\boldsymbol{y}_{1:t}) \propto p(\boldsymbol{y}_t|\boldsymbol{y}_{1:t-1}, \boldsymbol{\theta}) p(\boldsymbol{\theta}|\boldsymbol{y}_{1:t-1}). \tag{8}$$

However, the parameter likelihood $p(\boldsymbol{y}_t|\boldsymbol{y}_{1:t-1}, \boldsymbol{\theta})$ cannot be computed directly. Instead, we decompose it as

$$p(\boldsymbol{y}_t|\boldsymbol{y}_{1:t-1}, \boldsymbol{\theta}) = \int p(\boldsymbol{y}_t|\boldsymbol{x}_{0:t}, \boldsymbol{y}_{1:t-1}, \boldsymbol{\theta}) p(\boldsymbol{x}_{0:t}|\boldsymbol{y}_{1:t-1}, \boldsymbol{\theta}) d\boldsymbol{x}_{0:t}, \tag{9}$$

where $p(\boldsymbol{y}_t|\boldsymbol{x}_{0:t}, \boldsymbol{y}_{1:t-1}, \boldsymbol{\theta})$ and $p(\boldsymbol{x}_{0:t}|\boldsymbol{y}_{1:t-1}, \boldsymbol{\theta})$ are the likelihood and the predictive pdf of the state sequence $\boldsymbol{x}_{0:t}$, respectively, conditional on the previous observations and the parameters. These pdfs are computed in the second layer of the algorithm.

3.2. Second layer: slow states

Computations in this layer are conditional on the parameter vector $\boldsymbol{\theta}$. We seek to compute the smoothing posterior $p(\boldsymbol{x}_{0:t}|\boldsymbol{y}_{1:t}, \boldsymbol{\theta})$ as well as the predictive density $p(\boldsymbol{x}_{0:t}|\boldsymbol{y}_{1:t-1}, \boldsymbol{\theta})$ and the likelihood $p(\boldsymbol{y}_t|\boldsymbol{x}_{0:t}, \boldsymbol{y}_{1:t-1}, \boldsymbol{\theta})$, which are needed

Optimal filter

1st layer $\qquad\qquad$ 2nd layer $\qquad\qquad$ 3rd layer

Initialization

$p(\boldsymbol{\theta})$, $p(\boldsymbol{x}_0)$, $p(\boldsymbol{z}_0)$

$t-1$

$p(\boldsymbol{\theta}|\boldsymbol{y}_{1:t-1})$ $\qquad$ $p(\boldsymbol{x}_{0:t-1}|\boldsymbol{y}_{1:t-1},\boldsymbol{\theta})$ $\quad$ $p(\boldsymbol{z}_{h(t-2)+1:h(t-1)}|\boldsymbol{x}_{0:t-1},\boldsymbol{y}_{1:t-1},\boldsymbol{\theta})$ $\quad\leftarrow$ $\boldsymbol{y}_{t-1}$

t

Predictive pdf $\qquad$ a $\qquad$ Predictive pdf

$p(\boldsymbol{x}_{0:t}|\boldsymbol{y}_{1:t-1},\boldsymbol{\theta})$ $\qquad$ $p(\boldsymbol{z}_{h(t-1)+1:ht}|\boldsymbol{x}_{0:t-1},\boldsymbol{y}_{1:t-1},\boldsymbol{\theta})$

b

Likelihood $\qquad$ Likelihood $\qquad$ Likelihood $\qquad$ $\boldsymbol{y}_t$

$p(\boldsymbol{y}_t|\boldsymbol{y}_{1:t-1},\boldsymbol{\theta})$ $\quad$ $p(\boldsymbol{y}_t|\boldsymbol{x}_{0:t},\boldsymbol{y}_{1:t-1},\boldsymbol{\theta})$ $\quad$ $p(\boldsymbol{y}_t|\boldsymbol{z}_{ht},\boldsymbol{x}_t,\boldsymbol{\theta})$

Posterior $\qquad$ Posterior pdf $\qquad$ Posterior pdf

pdf $p(\boldsymbol{\theta}|\boldsymbol{y}_{1:t})$ $\quad$ $p(\boldsymbol{x}_{0:t}|\boldsymbol{y}_{1:t},\boldsymbol{\theta})$ $\quad$ $p(\boldsymbol{z}_{h(t-1)+1:ht}|\boldsymbol{x}_{0:t},\boldsymbol{y}_{1:t},\boldsymbol{\theta})$
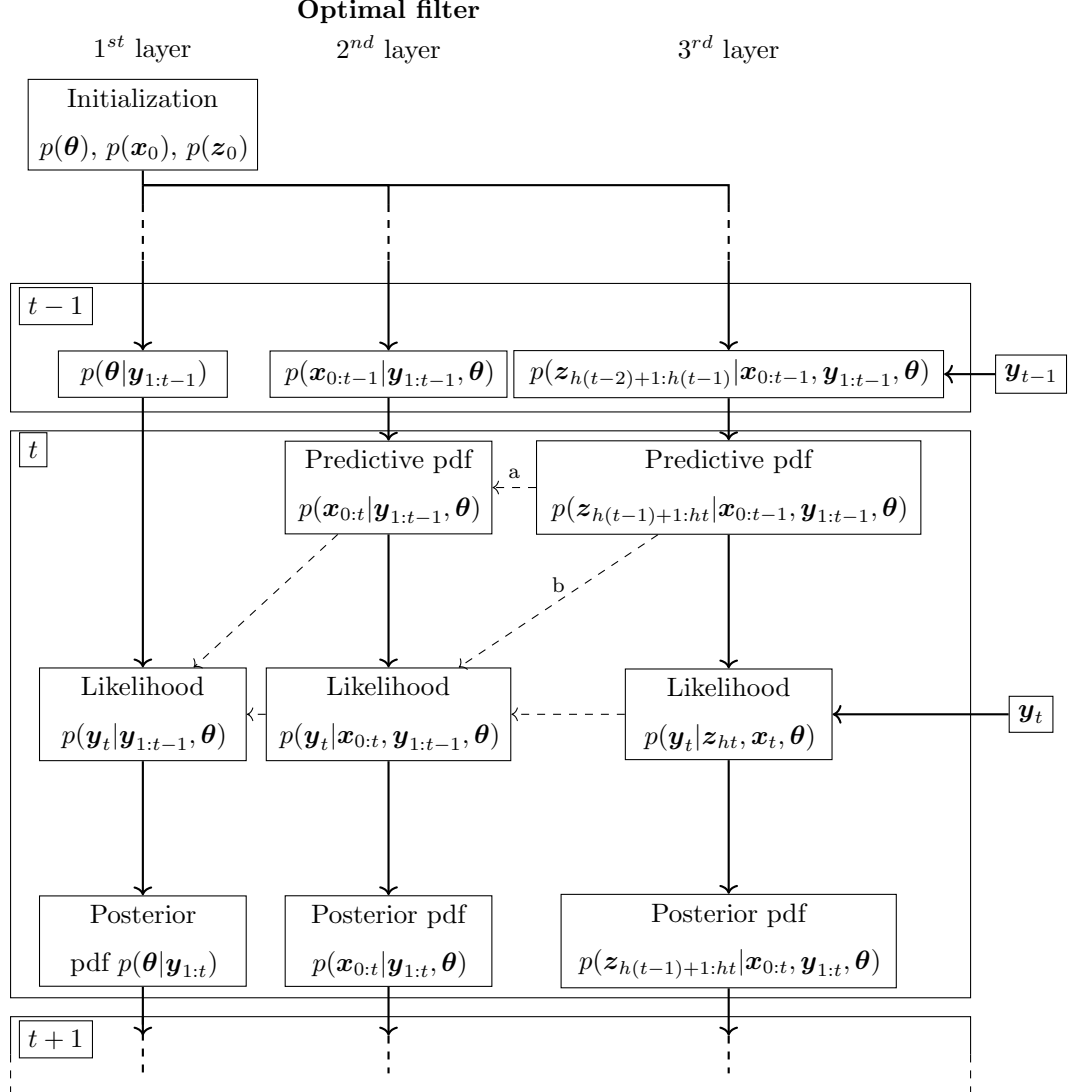
$t+1$

Figure 1: Schematic depiction of the optimal smoother. Each column represents a layer of computation and the dependencies among pdfs are indicated by arrows. The dashed arrows are used to show relations among different layers while the solid arrows represent dependencies in the same layer. Arrows a and b indicate that some intermediate computations are needed to relate both pdfs.

in the first layer –see Eq. (9). We assume that the prior density $p(\boldsymbol{x}_0)$ is known and the posterior pdf of the slow states at time $t-1$ (conditional on $\boldsymbol{\theta}$), $p(\boldsymbol{x}_{0:t-1}|\boldsymbol{y}_{1:t-1},\boldsymbol{\theta})$, is available at time t.

We first seek the predictive density of $\boldsymbol{x}_{0:t}$, namely,

$$p(\boldsymbol{x}_{0:t}|\boldsymbol{y}_{1:t-1},\boldsymbol{\theta}) = p(\boldsymbol{x}_t|\boldsymbol{x}_{0:t-1},\boldsymbol{y}_{1:t-1},\boldsymbol{\theta})p(\boldsymbol{x}_{0:t-1}|\boldsymbol{y}_{1:t-1},\boldsymbol{\theta}), \qquad (10)$$

which is obtained recursively from the posterior at time $t-1$, $p(\boldsymbol{x}_{0:t-1}|\boldsymbol{y}_{1:t-1},\boldsymbol{\theta})$, but requires the evaluation of the marginal density $p(\boldsymbol{x}_t|\boldsymbol{x}_{0:t-1},\boldsymbol{y}_{1:t-1},\boldsymbol{\theta})$. The latter is not directly available. It has to be computed as an integral with respect to (w.r.t.) the fast state variables, in particular

$$p(\boldsymbol{x}_t|\boldsymbol{x}_{0:t-1},\boldsymbol{y}_{1:t-1},\boldsymbol{\theta}) = \int p(\boldsymbol{x}_t|\boldsymbol{z}_{h(t-1)+1:ht},\boldsymbol{x}_{0:t-1},\boldsymbol{y}_{1:t-1},\boldsymbol{\theta})\times$$

$$\times p(\boldsymbol{z}_{h(t-1)+1:ht}|\boldsymbol{x}_{0:t-1},\boldsymbol{y}_{1:t-1},\boldsymbol{\theta})d\boldsymbol{z}_{h(t-1)+1:ht}. \quad (11)$$

The two densities in the integrand of Eq. (11), which involve the fast state variables $\boldsymbol{z}_{h(t-1)},\ldots,\boldsymbol{z}_{ht}$, are calculated in the third layer. Recall that h is the number of discrete-time steps of the fast states per each single time step of the slow variables (i.e., the $\boldsymbol{z}_n$'s are h time faster than the $\boldsymbol{x}_t$'s).

As for the likelihood, when $\boldsymbol{y}_t$ becomes available we update the posterior density of $\boldsymbol{x}_{0:t}$ (conditional on $\boldsymbol{\theta}$) as

$$p(\boldsymbol{x}_{0:t}|\boldsymbol{y}_{1:t},\boldsymbol{\theta}) \propto p(\boldsymbol{y}_t|\boldsymbol{x}_{0:t},\boldsymbol{y}_{1:t-1},\boldsymbol{\theta})p(\boldsymbol{x}_{0:t}|\boldsymbol{y}_{1:t-1},\boldsymbol{\theta}). \qquad (12)$$

In the equation above, the likelihood $p(\boldsymbol{y}_t|\boldsymbol{x}_{0:t},\boldsymbol{y}_{1:t-1},\boldsymbol{\theta})$ can be computed as an integral w.r.t. the fast state variables, specifically,

$$p(\boldsymbol{y}_t|\boldsymbol{x}_{0:t},\boldsymbol{y}_{1:t-1},\boldsymbol{\theta}) = \int p(\boldsymbol{y}_t|\boldsymbol{z}_{h(t-1)+1:ht},\boldsymbol{x}_{0:t},\boldsymbol{y}_{1:t-1},\boldsymbol{\theta})\times$$

$$\times \quad p(\boldsymbol{z}_{h(t-1)+1:ht}|\boldsymbol{x}_{0:t},\boldsymbol{y}_{1:t-1},\boldsymbol{\theta})d\boldsymbol{z}_{h(t-1)+1:ht}$$

$$= \int p(\boldsymbol{y}_t|\boldsymbol{z}_{ht},\boldsymbol{x}_t,\boldsymbol{\theta})p(\boldsymbol{z}_{h(t-1)+1:ht}|\boldsymbol{x}_{0:t},\boldsymbol{y}_{1:t-1},\boldsymbol{\theta})d\boldsymbol{z}_{h(t-1)+1:ht}.$$

$$(13)$$

The likelihood function $p(\boldsymbol{y}_t|\boldsymbol{z}_{ht},\boldsymbol{x}_t,\boldsymbol{\theta})$ can be obtained directly from the state-space model described by Eqs. (3)-(6), while the conditional pdf of the

subsequence $\boldsymbol{z}_{h(t-1)+1:ht}$ can be further decomposed as

$$
\begin{aligned}
p(\boldsymbol{z}_{h(t-1)+1:ht}|\boldsymbol{x}_{0:t}, \boldsymbol{y}_{1:t-1}, \boldsymbol{\theta}) \;=\; & \frac{p(\boldsymbol{x}_t|\boldsymbol{z}_{h(t-1)+1:ht}, \boldsymbol{x}_{t-1}, \boldsymbol{\theta})}{p(\boldsymbol{x}_t|\boldsymbol{x}_{0:t-1}, \boldsymbol{y}_{1:t-1}, \boldsymbol{\theta})} \\
& \times p(\boldsymbol{z}_{h(t-1)+1:ht}|\boldsymbol{x}_{0:t-1}, \boldsymbol{y}_{1:t-1}, \boldsymbol{\theta}). \quad (14)
\end{aligned}
$$

Both the likelihood $p(\boldsymbol{y}_t|\boldsymbol{x}_{0:t}, \boldsymbol{y}_{1:t-1}, \boldsymbol{\theta})$ of Eq. (13) and the predictive density $p(\boldsymbol{z}_{h(t-1)+1:ht}|\boldsymbol{x}_{0:t-1}, \boldsymbol{y}_{1:t-1}, \boldsymbol{\theta})$ of Eq. (14) are explicitly computed in the third layer.

3.3. Third layer: fast states

Computations on this layer are conditional on the parameter vector $\boldsymbol{\theta}$ and the sequence of slow states $\boldsymbol{x}_{0:t}$. In particular, we seek to compute the conditional posterior pdfs of $\boldsymbol{z}_{h(t-1)+1:ht}$, including the predictive densities,

$$
p(\boldsymbol{z}_{h(t-1)+1:ht}|\boldsymbol{x}_{0:t-1}, \boldsymbol{y}_{1:t-1}, \boldsymbol{\theta}) \quad \text{and} \quad p(\boldsymbol{z}_{h(t-1)+1:ht}|\boldsymbol{x}_{0:t}, \boldsymbol{y}_{1:t-1}, \boldsymbol{\theta}),
$$

as well as the updated density $p(\boldsymbol{z}_{h(t-1)+1:ht}|\boldsymbol{x}_{0:t}, \boldsymbol{y}_{1:t}, \boldsymbol{\theta})$. We also evaluate the plain likelihood function $p(\boldsymbol{y}_t|\boldsymbol{z}_{ht}, \boldsymbol{x}_t, \boldsymbol{\theta})$. We assume that the prior pdf of the fast states, $p(\boldsymbol{z})$, is known and the posterior up to time $t-1$, $p(\boldsymbol{z}_{h(t-2)+1:h(t-1)}|\boldsymbol{x}_{t-1}, \boldsymbol{y}_{1:t-1}, \boldsymbol{\theta})$, is available to enable recursive computations.

The first predictive pdf is computed recursively from the posterior up to time $t-1$ as the integral

$$
\begin{aligned}
p(\boldsymbol{z}_{h(t-1)+1:ht}|\boldsymbol{x}_{0:t-1}, \boldsymbol{y}_{1:t-1}, \boldsymbol{\theta}) \;=\; & \\
\int p(\boldsymbol{z}_{h(t-1)+1:ht}|\boldsymbol{z}_{h(t-2)+1:h(t-1)}, \boldsymbol{x}_{0:t-1}, \boldsymbol{y}_{1:t-1}, \boldsymbol{\theta}) \times & \\
\times p(\boldsymbol{z}_{h(t-2)+1:h(t-1)}|\boldsymbol{x}_{0:t-1}, \boldsymbol{y}_{1:t-1}, \boldsymbol{\theta}) d\boldsymbol{z}_{h(t-2)+1:h(t-1)} \;=\; & \\
\int p(\boldsymbol{z}_{h(t-1)+1:ht}|\boldsymbol{z}_{h(t-1)}, \boldsymbol{x}_{t-1}, \boldsymbol{\theta}) \times & \\
p(\boldsymbol{z}_{h(t-2)+1:h(t-1)}|\boldsymbol{x}_{0:t-1}, \boldsymbol{y}_{1:t-1}, \boldsymbol{\theta}) d\boldsymbol{z}_{h(t-2)+1:h(t-1)}, & \quad (15)
\end{aligned}
$$

where the transition pdf $p(\boldsymbol{z}_{h(t-1)+1:ht}|\boldsymbol{z}_{h(t-1)}, \boldsymbol{x}_{t-1}, \boldsymbol{\theta})$ is obtained immediately by iterating Eq. (3) in the state-space model h times and $p(\boldsymbol{z}_{h(t-2)+1:h(t-1)}|\boldsymbol{x}_{0:t-1}, \boldsymbol{y}_{1:t-1}, \boldsymbol{\theta}) d\boldsymbol{z}_{h(t-2)+1:h(t-1)}$ is the posterior pdf of the fast states in the previous time step. Besides, the second predictive density,

$p(\boldsymbol{z}_{h(t-1)+1:ht}|\boldsymbol{x}_{0:t},\boldsymbol{y}_{1:t-1},\boldsymbol{\theta})$, is obtained by substituting the first predictive pdf of Eq. (15) into Eq. (14)[1].

Finally, when the observation $\boldsymbol{y}_t$ becomes available, we compute the plain likelihood $p(\boldsymbol{y}_t|\boldsymbol{z}_{ht},\boldsymbol{x}_t,\boldsymbol{\theta})$ (from Eq. (6) in the state-space model) and then update the conditional posterior pdf of the fast state variables, namely,

$$p(\boldsymbol{z}_{h(t-1)+1:ht}|\boldsymbol{x}_{0:t},\boldsymbol{y}_{1:t},\boldsymbol{\theta}) = \frac{p(\boldsymbol{y}_t|\boldsymbol{z}_{ht},\boldsymbol{x}_t,\boldsymbol{\theta})p(\boldsymbol{x}_t|\boldsymbol{z}_{h(t-1)+1:ht},\boldsymbol{x}_{t-1},\boldsymbol{\theta})}{p(\boldsymbol{y}_t|\boldsymbol{x}_{0:t},\boldsymbol{y}_{1:t-1},\boldsymbol{\theta})p(\boldsymbol{x}_t|\boldsymbol{x}_{0:t-1},\boldsymbol{y}_{1:t-1},\boldsymbol{\theta})} \times$$
$$\times\, p(\boldsymbol{z}_{h(t-1)+1:ht}|\boldsymbol{x}_{0:t-1},\boldsymbol{y}_{1:t-1},\boldsymbol{\theta})$$

or, simply,

$$p(\boldsymbol{z}_{h(t-1)+1:ht}|\boldsymbol{x}_{0:t},\boldsymbol{y}_{1:t},\boldsymbol{\theta}) \propto p(\boldsymbol{y}_t|\boldsymbol{z}_{ht},\boldsymbol{x}_t,\boldsymbol{\theta})p(\boldsymbol{x}_t|\boldsymbol{z}_{h(t-1)+1:ht},\boldsymbol{x}_{t-1},\boldsymbol{\theta})\times$$
$$\times\, p(\boldsymbol{z}_{h(t-1)+1:ht}|\boldsymbol{x}_{0:t-1},\boldsymbol{y}_{1:t-1},\boldsymbol{\theta}) \qquad (16)$$

if we skip the normalization constant that is typically not needed explicitly for numerical implementations.

3.4. Outline of the optimal nested smoother

The optimal nested smoother uses each layer of computation to track a subset of r.v.s that evolve over their own time scale, by computing the corresponding predictive and updated pdfs (when observations are collected), as well as the necessary likelihoods. To be specific:

- The third layer tracks the fast state variables, $\boldsymbol{z}_n$, and computes the predictive pdf $p(\boldsymbol{z}_{h(t-1)+1:ht}|\boldsymbol{x}_{0:t-1},\boldsymbol{y}_{1:t-1},\boldsymbol{\theta})$ of Eq. (15) and the likelihood $p(\boldsymbol{y}_t|\boldsymbol{z}_{ht},\boldsymbol{x}_t,\boldsymbol{\theta})$. They are used to track the conditional posterior density $p(\boldsymbol{z}_{h(t-1)+1:ht}|\boldsymbol{x}_{0:t},\boldsymbol{y}_{1:t},\boldsymbol{\theta})$ of Eq. (16).

- The second layer takes the pdf $p(\boldsymbol{z}_{h(t-1)+1:ht}|\boldsymbol{x}_{0:t-1},\boldsymbol{y}_{1:t-1},\boldsymbol{\theta})$ and the likelihood $p(\boldsymbol{y}_t|\boldsymbol{z}_{ht},\boldsymbol{x}_t,\boldsymbol{\theta})$ in order to compute the predictive pdf

---

[1]Note that, in Eq. (14), the density $p(\boldsymbol{x}_t|\boldsymbol{x}_{0:t-1},\boldsymbol{y}_{1:t-1},\boldsymbol{\theta})$ is the normalization constant for the conditional pdf $p(\boldsymbol{z}_{h(t-1)+1:ht}|\boldsymbol{x}_{0:t-1},\boldsymbol{y}_{1:t-1},\boldsymbol{\theta})$, while $p(\boldsymbol{x}_t|\boldsymbol{z}_{h(t-1)+1:ht},\boldsymbol{x}_{t-1},\boldsymbol{\theta})$ results from the iteration of Eq. (3).

$p(\boldsymbol{x}_{0:t}|\boldsymbol{y}_{1:t-1}, \boldsymbol{\theta})$ in Eq. (10) and the likelihood $p(\boldsymbol{y}_t|\boldsymbol{x}_{0:t}, \boldsymbol{y}_{1:t-1}, \boldsymbol{\theta})$ in Eq. (13). These are used to track the posterior pdf of the slow state, $p(\boldsymbol{x}_{0:t}|\boldsymbol{y}_{1:t}, \boldsymbol{\theta})$, of Eq. (12).

- The first layer takes the pdfs $p(\boldsymbol{x}_{0:t}|\boldsymbol{y}_{1:t-1}, \boldsymbol{\theta})$ and $p(\boldsymbol{y}_t|\boldsymbol{x}_{0:t}, \boldsymbol{y}_{1:t-1}, \boldsymbol{\theta})$ to track the posterior pdf of the parameters, $p(\boldsymbol{\theta}|\boldsymbol{y}_{1:t})$, of Eq. (8).

Finally, the three conditional posterior pdfs are needed to compute the joint smoothing density $p(\boldsymbol{z}_{h(t-1)+1:ht}, \boldsymbol{x}_{0:t}, \boldsymbol{\theta}|\boldsymbol{y}_{1:t})$ in Eq. (7).

Figure 1 is a schematic representation of the optimal smoother, which displays each layer in a different column. Most of the pdfs that need to be computed are included in this scheme, showing the dependencies among them with arrows. These relations are direct except for the arrows labeled a and b, which require one or more intermediate computations. In the case of arrow a, the predictive pdf $p(\boldsymbol{z}_{h(t-1)+1:ht}|\boldsymbol{x}_{0:t-1}, \boldsymbol{y}_{1:t-1}, \boldsymbol{\theta})$ is used to compute $p(\boldsymbol{x}_t|\boldsymbol{x}_{0:t-1}, \boldsymbol{y}_{1:t-1}, \boldsymbol{\theta})$ in Eq. (11), that is necessary to calculate the predictive density $p(\boldsymbol{x}_{0:t}|\boldsymbol{y}_{1:t-1}, \boldsymbol{\theta})$ of the second layer in Eq. (10). As for the arrow labeled b, the predictive density $p(\boldsymbol{z}_{h(t-1)+1:ht}|\boldsymbol{x}_{0:t-1}, \boldsymbol{y}_{1:t-1}, \boldsymbol{\theta})$ is used to compute the pdf $p(\boldsymbol{z}_{h(t-1)+1:ht}|\boldsymbol{x}_{0:t}, \boldsymbol{y}_{1:t-1}, \boldsymbol{\theta})$ in Eq. (14), that is used, in turn, to obtain the likelihood $p(\boldsymbol{y}_t|\boldsymbol{x}_{0:t}, \boldsymbol{y}_{1:t-1}, \boldsymbol{\theta})$ in Eq. (13).

4. Approximate smoothing algorithms

The optimal algorithm described in Section 3 cannot be implemented exactly for most practical models. Instead, one needs to devise suitable approximations that can be implemented numerically in an efficient way. One possible approach is a full-blown SMC implementation that extends the nested particle filter of [8]. However, such a scheme with three layers of computation results in a prohibitive computational cost. Instead, we introduce herein two different algorithms that combine SMC and Gaussian approximations at the different layers. The resulting algorithms can be implemented numerically in a more efficient manner and are suitable for parallelization, which leads to very fast runtimes.

The first method involves using SMC schemes both at the first and second layer, together with a bank of unscented Kalman filters (UKFs) [15, 20] to approximate (as Gaussians) the conditional densities to be computed at the third layer. This implementation has great potential for parallelization, but it is computationally costly nevertheless. Hence, we also introduce a second, less demanding scheme that utilizes the same SMC scheme at the first layer but employs EnKFs [12] at the second layer and simple EKFs [2] to approximate the densities needed in the second and third layer, respectively. A numerical study of performance is carried out in Section 5 for both implementations.

4.1. First scheme

We introduce a numerical approximate smoother where the probability measures $p(\boldsymbol{\theta}|\boldsymbol{y}_{1:t})d\boldsymbol{\theta}$ and $p(\boldsymbol{x}_{0:t}|\boldsymbol{y}_{1:t}, \boldsymbol{\theta})d\boldsymbol{x}_{0:t}$ are approximated using SMC while we replace the conditional smoothing pdf $p(\boldsymbol{z}_{h(t-1)+1:ht}|\boldsymbol{x}_{0:t}, \boldsymbol{y}_{1:t}, \boldsymbol{\theta})$ by a sequence of Gaussian approximations of the densities $p(\boldsymbol{z}_n|\boldsymbol{x}_{0:t}, \boldsymbol{y}_{1:t}, \boldsymbol{\theta})$, for $n = h(t-1) + 1, \ldots, ht$, computed using a bank of UKFs.

First layer. Algorithm 1 describes the first layer of the nested smoother, which aims at the approximation of the posterior distribution of the parameters. It receives as inputs the prior pdfs of the parameters, $p(\boldsymbol{\theta})$, and the two subsets of state variables, $p(\boldsymbol{x}_0)$ and $p(\boldsymbol{z}_0)$. In the initialization step, they are used to generate starting Monte Carlo particles (for the SMC schemes) and sigma-points (for the UKFs) needed at each layer. Specifically, we generate N parameter samples $\{\boldsymbol{\theta}_0^i\}_{1 \leq i \leq N}$, J slow state particles per each parameter sample, $\{\boldsymbol{x}_0^{i,j}\}_{1 \leq j \leq J}$, and L sigma-points of the fast state per each slow state sample, $\{\boldsymbol{z}_0^{i,j,l}\}_{0 \leq l \leq L-1}$, to obtain a set of the form $\{\boldsymbol{\theta}_0^i, \{\boldsymbol{x}_0^{i,j}, \{\boldsymbol{z}_0^{i,j,l}\}_{0 \leq l \leq L-1}\}_{1 \leq j \leq J}\}_{1 \leq i \leq N}$. All particles are independent at time $t = n = 0$, provided the priors are independent.

Additionally, a Markov kernel $\kappa_N^{\boldsymbol{\theta}'}(d\boldsymbol{\theta})$ is needed for the jittering of parameter samples [8], i.e., to draw a new set of particles, $\{\bar{\boldsymbol{\theta}}_t^i\}_{1 \leq i \leq N}$, at each discrete-time step. This is needed to preserve the diversity of the particles, otherwise after

a few resampling steps the parameter particles would be reduced to just a few distinct values and the filter would collapse.

At every time step t (in the slow time scale), we compute the approximate likelihood for each particle $\bar{\boldsymbol{\theta}}_t^i$, namely

$$\hat{p}^{J,L}(\boldsymbol{y}_t|\boldsymbol{y}_{1:t-1},\bar{\boldsymbol{\theta}}_t^i) \approx p(\boldsymbol{y}_t|\boldsymbol{y}_{1:t-1},\bar{\boldsymbol{\theta}}_t^i),$$

in order to obtain the non-normalized weights $\{\tilde{v}_t^i\}_{1\leq i\leq N}$. The superscripts J and L indicate the dependence of the approximation on the number of particles generated for the second layer (J) and the number of sigma-points employed by the UKFs in the third layer (L). The states $\{\boldsymbol{x}_{t-1}^{i,j}, \{\boldsymbol{z}_{h(t-1)}^{i,j,l}\}_{0\leq l\leq L-1}\}_{1\leq j\leq J}$ are propagated to time t in the nested layers of filtering in step 2b. Finally, we normalize the weights in order to resample not only the parameter particles $\bar{\boldsymbol{\theta}}_t^i$, but also their associated sets of state variables.

Algorithm 1. *SMC approximation of $p(\boldsymbol{\theta}|\boldsymbol{y}_{1:t})$ in the first method*

    Inputs

- *Prior distributions $p(\boldsymbol{\theta})$, $p(\boldsymbol{x}_0)$ and $p(\boldsymbol{z}_0)$.*

- *A Markov kernel $\kappa_N^{\boldsymbol{\theta}'}(d\boldsymbol{\theta})$ which, given $\boldsymbol{\theta}'$, generates jittered parameters $\boldsymbol{\theta} \in \mathbb{R}^{d_\theta}$.*

    Initialization: *this is a joint initialization for all three layers.*

- *Draw N i.i.d. sample $\boldsymbol{\theta}_0^i$, $i = 1,\ldots,N$ from the prior distribution $p(\boldsymbol{\theta})$.*

- *Draw J i.i.d. samples $\boldsymbol{x}_0^{i,j}$, $i = 1,\ldots,N$, $j = 1,\ldots,J$, from the prior distribution $p(\boldsymbol{x}_0)$.*

- *Compute $L = 2d_z+1$ sigma-points, $\boldsymbol{z}_0^{i,j,l}$, with their respective weights, $\lambda_0^{i,j,l}$, $i = 1,\ldots,N$, $j = 1,\ldots,J$, $l = 0,\ldots,L-1$, from the prior distribution*

$p(\boldsymbol{z}_0|\hat{\boldsymbol{z}}_0, \boldsymbol{C}_0(\boldsymbol{z}))$ *as*

$$\boldsymbol{z}_0^{i,j,0} = \hat{\boldsymbol{z}}_0, \qquad\qquad \lambda_0^{i,j,0} = \frac{1}{1+d_z},$$

$$\boldsymbol{z}_0^{i,j,l} = \hat{\boldsymbol{z}}_0 + \boldsymbol{S}_l, \qquad\qquad \lambda_0^{i,j,l} = \frac{1 - \lambda_0^{i,j,0}}{2d_z},$$

$$\boldsymbol{z}_0^{i,j,l+d_z} = \hat{\boldsymbol{z}}_0 - \boldsymbol{S}_l, \qquad\qquad \lambda_0^{i,j,l+d_z} = \frac{1 - \lambda_0^{i,j,0}}{2d_z},$$

for $l = 1, \ldots, d_z$, where $\boldsymbol{S}_l$ is the l-th row or column of the matrix square root of $\frac{d_z}{1-\lambda_0^{i,j,0}} \boldsymbol{C}_0(\boldsymbol{z})$.

Procedure *For $t \geq 0$:*

1. *Draw N i.i.d samples $\bar{\boldsymbol{\theta}}_t^i$ from $\kappa_N^{\boldsymbol{\theta}_{t-1}^i}(d\boldsymbol{\theta})$.*

2. *For $i = 1, \ldots, N$:*

    (a) *Compute*
    $$\tilde{v}_t^i = \hat{p}^{J,L}(\boldsymbol{y}_t|\boldsymbol{y}_{1:t-1}, \bar{\boldsymbol{\theta}}_t^i), \tag{17}$$

    where the approximate likelihood is evaluated at layer 2.

    (b) *Obtain new particles $\{\boldsymbol{x}_t^{i,j}, \{\boldsymbol{z}_{ht}^{i,j,l}\}_{0 \leq l \leq L-1}\}_{1 \leq j \leq J}$ at time t (from layers 2 and 3).*

    (c) *Normalize the weights*
    $$v_t^i = \frac{\tilde{v}_t^i}{\sum_{i=1}^N \tilde{v}_t^i}. \tag{18}$$

3. *Resample: set for each $m = 1, \ldots, N$ and with probability v_t^i*

$$\{\boldsymbol{\theta}_t^m, \{\boldsymbol{x}_t^{(m,j)}, \{\boldsymbol{z}_{ht}^{m,j,l}\}_{0 \leq l \leq L-1}\}_{1 \leq j \leq J}\} = \{\bar{\boldsymbol{\theta}}_t^i, \{\boldsymbol{x}_t^{(i,j)}, \{\boldsymbol{z}_{ht}^{i,j,l}\}_{0 \leq l \leq L-1}\}_{1 \leq j \leq J}\}. \tag{19}$$

Outputs: $\{\boldsymbol{\theta}_t^i, \{\boldsymbol{x}_t^{(i,j)}, \{\boldsymbol{z}_{ht}^{i,j,l}\}\}_{1 \leq j \leq J}\}_{1 \leq i \leq N}$.

Second layer. Algorithm 2 describes the implementation of a bank of conditional SMC schemes in the second layer of the multi-scale nested smoother, one for each particle $\bar{\boldsymbol{\theta}}_t^i$, $i = 1, \ldots, N$. In this second layer we approximate the posterior distribution with density $p(\boldsymbol{x}_{0:t}|\boldsymbol{y}_{1:t}, \bar{\boldsymbol{\theta}}_t^i)$. The procedure is similar to the one in Algorithm 1, starting with the generation of the particles $\bar{\boldsymbol{x}}_t^{i,j}$, $j = 1, \ldots, J$, the computation of the approximate likelihood

$$\hat{p}^L(\boldsymbol{y}_t|\bar{\boldsymbol{x}}_t^{i,j}, \boldsymbol{x}_{0:t-1}^{i,j}, \boldsymbol{y}_{1:t-1}, \bar{\boldsymbol{\theta}}_t^i) \approx p(\boldsymbol{y}_t|\bar{\boldsymbol{x}}_t^{i,j}, \boldsymbol{x}_{0:t-1}^{i,j}, \boldsymbol{y}_{1:t-1}, \bar{\boldsymbol{\theta}}_t^i)$$

and the non-normalized weights $\{\tilde{u}_t^{i,j}\}_{1 \leq j \leq J}$ in step 1a. By averaging the latter weights we can obtain $\tilde{v}_t^i$ for its use in the first layer[2]. After propagating the fast state variables in the third layer (as described below), one can resample the set $\{\boldsymbol{x}_{0:t}^{i,j}, \{\boldsymbol{z}_{ht}^{i,j,l}\}_{0 \leq l \leq L-1}\}_{1 \leq j \leq J}$ using the normalized weights $\{u_t^{i,j}\}_{j=1}^J$ obtained in step 1c.

Third layer. Algorithm 3 outlines the implementation of a bank of UKFs [15] conditional on each parameter sample $\bar{\boldsymbol{\theta}}_t^i$ and the set of slow states $\{\bar{\boldsymbol{x}}_t^{i,j}\} \cup \boldsymbol{x}_{0:t-1}^{i,j}$. If we follow the template of the optimal smoother, then we should seek an approximation of the density $p(\boldsymbol{z}_{h(t-1)+1:ht}|\boldsymbol{x}_{0:t-1}^{i,j}, \boldsymbol{y}_{1:t-1}, \bar{\boldsymbol{\theta}}_t^i)$. However, performing this calculation with a UKF-like scheme implies that the dimension of the filter should be $d_z \times h$, in order to include the whole subsequence of states $\boldsymbol{z}_{h(t-1)+1:ht}$. Such approach would demand $2d_z h + 1$ sigma-points for each conditional UKF algorithm, and the computation of NJL covariance matrices with dimension $2d_z h \times 2d_z h$ each, which is impractical even for moderate d_z and h. For simplicity, in order to avoid operations with large matrices, we choose to compute Gaussian approximations of the marginal predictive densities $p(\boldsymbol{z}_q|\boldsymbol{x}_{0:t-1}^{i,j}, \boldsymbol{y}_{1:t-1}, \bar{\boldsymbol{\theta}}_t^i)$, for $q = h(t-1)+1, \ldots, ht$, and then use these marginals to estimate the average of the fast states $\bar{\boldsymbol{z}}_t$ which is necessary in the micro-macro solver of Eq. (3). The complete procedure is outlined in Algorithm 3, with further details below.

---

[2]The average $\tilde{v}_t^i = \frac{1}{J} \sum_{j=1}^J \tilde{u}_t^{i,j}$ is an approximation of the integral of Eq. (9).

Step 1 of Algorithm 3 generates new sigma-points in the space of fast states, $\breve{z}_q^{i,j,l}$, for $q = h(t-1) + 1, \ldots, ht$ and $l = 0, \ldots, L-1$, conditional on the parameters $\bar{\theta}_t^i$ and slow variables $x_{t-1}^{i,j}$. At each time q, we compute a predictive mean and a covariance matrix as

$$\breve{z}_q^{i,j} = \sum_{l=0}^{L-1} \lambda_{q-1}^{i,j,l} \tilde{z}_q^{i,j,l} \quad \text{and} \tag{20}$$

$$\check{C}_q^{i,j}(z) = \sum_{l=0}^{L-1} \lambda_{q-1}^{i,j,l} (\tilde{z}_q^{i,j,l} - \breve{z}_q^{i,j})(\tilde{z}_q^{i,j,l} - \breve{z}_q^{i,j})^\top + \Delta_z Q_z, \tag{21}$$

where the $\lambda_{q-1}^{i,j,l}$'s are the weights[3] of the sigma points $\breve{z}_{q-1}^{i,j,l}$ and $\Delta_z Q_z$ is the covariance matrix of the noise in Eq. (4). The mean in Eq. (20) and the covariance in Eq. (21) yield the approximation

$$\mathcal{N}(z_q | \breve{z}_q^{i,j}, \check{C}_q^{i,j}(z)) \approx p(z_q | x_{0:t-1}^{i,j}, y_{1:t-1}, \bar{\theta}_t^i) \tag{22}$$

and we compute a new weighted set of sigma-points $\{\breve{z}_q^{i,j,l}, \lambda_q^{i,j,l}\}$ to represent the Gaussian density in Eq. (22).

Algorithm 2. *SMC approximation of $p(x_{0:t} | y_{1:t}, \theta)$*

   Inputs

     - *Known parameter $\bar{\theta}_t^i$ and known initial states, $x_{t-1}^{i,j}$ and $z_{h(t-1)}^{i,j,l}$, for $j = 1, \ldots, J$ and $l = 0, \ldots, L-1$.*

   Procedure *For $t \geq 0$:*

   1. For $j = 1, \ldots, J$:

     (a) Compute

$$\tilde{u}_t^{i,j} = \hat{p}^L(y_t | \bar{x}_t^{i,j}, x_{0:t-1}^{i,j}, y_{1:t-1}, \bar{\theta}_t^i), \tag{23}$$

$$\tilde{v}_t^i = \frac{1}{J} \sum_{j=1}^{J} \tilde{u}_t^{i,j}, \tag{24}$$

---

[3]These weights are deterministic and can be computed a priori in different ways. See [20] for a survey of methods.

where the new particle $\bar{\boldsymbol{x}}_t^{i,j}$ is generated, and the approximate likelihood is evaluated, at layer 3.

(b) Obtain new particles $\{\boldsymbol{z}_{ht}^{i,j,l}\}_{0 \leq l \leq L-1}$ at time t, from layer 3.

(c) Normalize the weights

$$u_t^{i,j} = \frac{\tilde{u}_t^{i,j}}{\sum_{j=1}^{J} \tilde{u}_t^{i,j}}. \tag{25}$$

2. Resample: set

$$\{\boldsymbol{x}_t^{i,m}, \{\boldsymbol{z}_{ht}^{i,m,l}\}_{0 \leq l \leq L-1}\} = \{\bar{\boldsymbol{x}}_t^{i,j}, \{\boldsymbol{z}_{ht}^{i,j,l}\}_{0 \leq l \leq L-1}\} \tag{26}$$

with probability $u_t^{i,j}$ for each $m = 1, \ldots, J$.

Outputs: $\{\boldsymbol{x}_t^{i,j}, \{\boldsymbol{z}_{ht}^{i,j,l}\}_{0 \leq l \leq L-1}\}_{1 \leq j \leq J}$ and $\tilde{v}_t^i$.

Algorithm 3. *UKF approximation of* $p(\boldsymbol{z}_{h(t-1)+1:ht}|\boldsymbol{x}_{0:t}, \boldsymbol{y}_{1:t}, \boldsymbol{\theta})$

   Inputs

   - *Integration steps* Δ_x, Δ_z *and time scale ratio* $h = \frac{\Delta_x}{\Delta_z} \in \mathbb{Z}^+$.

   - *Known parameter vector* $\bar{\boldsymbol{\theta}}_t^i$ *and initial slow state* $\boldsymbol{x}_{t-1}^{i,j}$. *Weighted sigma-points for the fast state at time* $h(t-1)$, *denoted* $\{\boldsymbol{z}_{h(t-1)}^{i,j,l}, \lambda_{h(t-1)}^{i,j,l}\}_{l=0}^{L-1}$.

   Procedure *For* $t > 0$:

1. *Set* $\check{\boldsymbol{z}}_{h(t-1)}^{i,j,l} = \boldsymbol{z}_{h(t-1)}^{i,j,l}$. *For* $l = 0, \ldots, L-1$ *and for* $q = h(t-1)+1, \ldots, ht$:

   (a) *Integrate with step* Δ_z

$$\check{\boldsymbol{z}}_q^{i,j,l} = \check{\boldsymbol{z}}_{q-1}^{i,j,l} + \Delta_z(f_{\boldsymbol{z}}(\check{\boldsymbol{z}}_{q-1}^{i,j,l}, \bar{\boldsymbol{\theta}}_t^i) + g_{\boldsymbol{z}}(\boldsymbol{x}_{t-1}^{i,j}, \bar{\boldsymbol{\theta}}_t^i)), \tag{27}$$

   and compute the predictive mean, $\check{\boldsymbol{z}}_q^{i,j}$, *and the predictive covariance matrix,* $\check{\boldsymbol{C}}_q^{i,j}(\boldsymbol{z})$, *using Eqs.* (20) *and* (21).

(b) *Approximate the predictive pdf of the fast states as Gaussian density,*

$$p(\boldsymbol{z}_q | \boldsymbol{x}_{0:t-1}^{i,j}, \boldsymbol{y}_{1:t-1}, \bar{\boldsymbol{\theta}}_t^i) \approx \mathcal{N}(\boldsymbol{z}_q | \check{\boldsymbol{z}}_q^{i,j}, \check{\boldsymbol{C}}_q^{i,j}(\boldsymbol{z})).$$

Represent this Gaussian distribution by a set of weighted sigma-points denoted $\{\check{\boldsymbol{z}}_q^{i,j,l}, \lambda_q^{i,j,l}\}_{l=0}^{L-1}$.

2. *In the space of the slow state variables:*

(a) *For $l = 0, \ldots, L-1$, project the sigma-points $\check{\boldsymbol{z}}_{h(t-1)+1:ht}^{i,j,l}$ to obtain sigma-points in the space of the slow states,*

$$\tilde{\boldsymbol{x}}_t^{i,j,l} = \boldsymbol{x}_{t-1}^{i,j} + \Delta_x(f_{\boldsymbol{x}}(\boldsymbol{x}_{t-1}^{i,j}, \bar{\boldsymbol{\theta}}_t^i) + g_{\boldsymbol{x}}(\bar{\boldsymbol{z}}_t^{i,j,l}, \bar{\boldsymbol{\theta}}_t^i)), \qquad (28)$$

where $\bar{\boldsymbol{z}}_t^{i,j,l} = \frac{1}{h} \sum_{q=h(t-1)+1}^{ht} \check{\boldsymbol{z}}_q^{i,j,l}$. Then, compute a mean vector $\check{\boldsymbol{x}}_t^{i,j}$ and a covariance matrix $\check{\boldsymbol{C}}_t^{i,j}(\boldsymbol{x})$ using Eqs. (34) and (35).

(b) *Sample $\bar{\boldsymbol{x}}_t^{i,j} \sim \mathcal{N}(\boldsymbol{x}_t | \check{\boldsymbol{x}}_t^{i,j}, \check{\boldsymbol{C}}_t^{i,j}(\boldsymbol{x}))$.*

3. *Once we collect a new observation $\boldsymbol{y}_t$,*

(a) *For $l = 0, \ldots, L-1$, project the sigma-points $\check{\boldsymbol{z}}_{ht}^{i,j,l}$ and the new sample $\bar{\boldsymbol{x}}_t^{i,j}$ into the observation space,*

$$\tilde{\boldsymbol{y}}_t^{i,j,l} = l(\check{\boldsymbol{z}}_{ht}^{i,j,l}, \bar{\boldsymbol{x}}_t^{i,j}, \bar{\boldsymbol{\theta}}_t^i), \qquad (29)$$

then compute the mean vector $\hat{\boldsymbol{y}}_{ht}^{i,j}$ and the covariance matrix $\boldsymbol{C}_t^{i,j}(\boldsymbol{y})$ using Eqs. (36) and (37).

(b) *Compute $\tilde{w}_t^{i,j,l} = p(\boldsymbol{y}_t | \check{\boldsymbol{z}}_{ht}^{i,j,l}, \bar{\boldsymbol{x}}_t^{i,j}, \bar{\boldsymbol{\theta}}_t^i) p(\bar{\boldsymbol{x}}_t^{i,j} | \check{\boldsymbol{z}}_{h(t-1)+1:ht}^{i,j,l}, \boldsymbol{x}_{t-1}^{i,j}, \bar{\boldsymbol{\theta}}_t^i)$ and the weights for the second layer*

$$\tilde{u}_t^{i,j} = \sum_{l=0}^{L-1} \lambda_{ht}^{i,j,l} \tilde{w}_t^{i,j,l}. \qquad (30)$$

4. *Update the mean and the covariance matrix of the fast variables*

$$\boldsymbol{K}_t(\boldsymbol{z}) = \boldsymbol{C}_t^{i,j}(\boldsymbol{z}, \boldsymbol{y})\big(\boldsymbol{C}_t^{i,j}(\boldsymbol{y})\big)^{-1}, \qquad (31)$$

$$\hat{\boldsymbol{z}}_{ht}^{i,j} = \check{\boldsymbol{z}}_{ht}^{i,j} + \boldsymbol{K}_t(\boldsymbol{z})\big(\boldsymbol{y}_t - \hat{\boldsymbol{y}}_t^{i,j}\big) \quad and \qquad (32)$$

$$\hat{\boldsymbol{C}}_{ht}^{i,j}(\boldsymbol{z}) = \check{\boldsymbol{C}}_{ht}^{i,j}(\boldsymbol{z}) + \boldsymbol{K}_t(\boldsymbol{z})\boldsymbol{C}_t^{i,j}(\boldsymbol{y})\big(\boldsymbol{K}_t(\boldsymbol{z})\big)^{\top}, \qquad (33)$$

where $\boldsymbol{C}_t^{i,j}(\boldsymbol{z}, \boldsymbol{y})$ is the cross-covariance matrix computed in Eq. (38).

5. *From the new Gaussian pdf $\mathcal{N}(z_{ht}|\hat{z}_{ht}^{i,j}, \hat{C}_t^{i,j}(z))$, generate $L = 2d_z + 1$ sigma-points and weights $\{z_{ht}^{i,j,l}, \lambda_{ht}^{i,j,l}\}_{0 \le l \le L-1}$.*

Outputs: $\{z_{ht}^{i,j,l}\}_{0 \le l \le L-1}$, $\bar{x}_t^{i,j}$ *and* $\tilde{u}_t^{i,j}$.

In step 2 of Algorithm 3 we use the sigma-points at time $q = ht$ to generate new particles for the slow states at time t. Specifically, we project the $\check{z}_{ht}^{i,j,l}$'s through the state equation of the slow state variables to obtain sigma-points in the space of the slow variables, denoted $\tilde{x}_t^{i,j,l}$. From these sigma-points, we obtain a mean vector and a covariance matrix, respectively,

$$\check{x}_t^{i,j} = \sum_{l=0}^{L-1} \lambda_{ht}^{i,j,l} \tilde{x}_t^{i,j,l} \quad \text{and} \tag{34}$$

$$\check{C}_t^{i,j}(x) = \sum_{l=0}^{L-1} \lambda_{ht}^{i,j,l} (\tilde{x}_t^{i,j,l} - \check{x}_t^{i,j})(\tilde{x}_t^{i,j,l} - \check{x}_t^{i,j})^\top + \Delta_x Q_x, \tag{35}$$

where $\Delta_x Q_x$ is the covariance matrix of the noise in Eq. (3). Eqs. (34) and (35) yield a Gaussian approximation of the predictive pdf of the slow states, namely,

$$p(x_t|x_{0:t-1}^{i,j}, y_{0:t-1}, \bar{\theta}_t^i) \approx \mathcal{N}(x|\check{x}_t^{i,j}, \check{C}_t^{i,j}(x)).$$

We generate the new particle $\bar{x}_t^{i,j}$ from this Gaussian density.

In step 3 of the algorithm we propagate the sigma-points $\check{z}_{ht}^{i,j,l}$ and the particle $\bar{x}_t^{i,j}$ through the observation function $l(\cdot)$ to obtain projected sigma-points (on the observation space) $\{\tilde{y}_t^{i,j,l}\}_{0 \le l \le L-1}$. We use these projected sigma-points to obtain a predictive mean and covariance matrix for the observation y_t, namely,

$$\hat{y}_t^{i,j} = \sum_{l=0}^{L-1} \lambda_{ht}^{i,j,l} \tilde{y}_t^{i,j,l} \quad \text{and} \tag{36}$$

$$C_t^{i,j}(y) = \sum_{l=0}^{L-1} \lambda_{ht}^{i,j,l} (\tilde{y}_t^{i,j,l} - \hat{y}_t^{i,j})(\tilde{y}_t^{i,j,l} - \hat{y}_t^{i,j})^\top + R, \tag{37}$$

where R is the covariance matrix of the noise in the observation equation. At this step we also compute the non-normalized importance weight $\tilde{u}_t^{i,j}$ which is output to layer 2.

In step 4, we compute the Kalman gain using the observation covariance matrix of Eq. (37) and the cross-covariance matrix

$$\boldsymbol{C}_t^{i,j}(\boldsymbol{z}, \boldsymbol{y}) = \sum_{l=0}^{L-1} \lambda_{ht}^{i,j,l} (\check{\boldsymbol{z}}_{ht}^{i,j,l} - \check{\boldsymbol{z}}_{ht}^{i,j})(\tilde{\boldsymbol{y}}_t^{i,j,l} - \hat{\boldsymbol{y}}_t^{i,j})^\top. \tag{38}$$

Then we update the mean, $\hat{\boldsymbol{z}}_{ht}^{i,j}$, and covariance matrix, $\hat{\boldsymbol{C}}_{ht}^{i,j}(\boldsymbol{z})$, of the fast state variables to obtain the approximation

$$p(\boldsymbol{z}_{ht}|\bar{\boldsymbol{x}}_t^{i,j}, \boldsymbol{x}_{0:t-1}^{i,j}, \boldsymbol{y}_{1:t}, \bar{\boldsymbol{\theta}}_t^i) \approx \mathcal{N}(\boldsymbol{z}_{ht}|\hat{\boldsymbol{z}}_{ht}^{i,j}, \hat{\boldsymbol{C}}_{ht}^{i,j}(\boldsymbol{z})). \tag{39}$$

Finally, in step 5 we generate new weighted sigma-points to characterize the Gaussian pdf in Eq. (39).

4.2. Second scheme

The method in Section 4.1 may still have a prohibitive computational cost, as it generates a total of $N \times J \times L$ particles in the joint space of the parameters, the slow states and the fast states (if we count sigma-points as deterministic particles). In this section we describe a computationally-lighter procedure that replaces the SMC procedure in layer 2 by an EnKF [12] and the UKF in layer 3 by a simpler EKF [2]. The complete procedure is described below.

First layer. We describe the use of a SMC algorithm for the first layer of the nested algorithm in order to approximate $p(\boldsymbol{\theta}|\boldsymbol{y}_{1:t})$. This is the same as in Algorithm 1, except that we need to take into account the initializations needed for layers 2 and 3. Algorithm 4 receives as inputs the prior distributions of the parameters, $p(\boldsymbol{\theta})$, and both subsets of state variables, $p(\boldsymbol{x}_0)$ and $p(\boldsymbol{z}_0)$. They are used to generate

- the initial particles from $p(\boldsymbol{\theta})$ for the SMC scheme, denoted $\{\boldsymbol{\theta}_0^i\}_{i=1}^N$,

- the samples from $p(\boldsymbol{x}_0)$ utilized to build the ensembles $\boldsymbol{X}_0^i$, $i = 1, \ldots, N$, for the EnKFs in the second layer,

- and the mean and covariance matrix of $\boldsymbol{z}$ for the EKFs in the third layer, denoted $\boldsymbol{z}_0^{i,j} = \mathbb{E}[\boldsymbol{z}_0]$ and $\boldsymbol{C}_0^{i,j}(\boldsymbol{z}) = \text{Cov}(\boldsymbol{z}_0)$, respectively (note that they are the same for all i and j).

23

The rest of the procedure is the same as in Algorithm 1.

Second layer. In Algorithm 5 we employ an EnKF to obtain ensemble approximations of $p(\boldsymbol{x}_t|\boldsymbol{y}_{1:t-1}, \bar{\boldsymbol{\theta}}_t^i)$ and $p(\boldsymbol{x}_t|\boldsymbol{y}_{1:t}, \bar{\boldsymbol{\theta}}_t^i)$. The ensembles are denoted $\bar{\boldsymbol{X}}_t^i$ and $\boldsymbol{X}_t^i$, respectively, and they are used to approximate the computations that involved the joint pdfs $p(\boldsymbol{x}_{0:t}|\boldsymbol{y}_{1:t-1}, \bar{\boldsymbol{\theta}}_t^i)$ and $p(\boldsymbol{x}_{0:t}|\boldsymbol{y}_{1:t}, \bar{\boldsymbol{\theta}}_t^i)$ in the optimal smoother. Note that all calculations are conditional on the i-th parameter particle, $\bar{\boldsymbol{\theta}}_t^i$.

The scheme is similar to Algorithm 2. At step 1a, we retrieve the new samples $\bar{\boldsymbol{x}}_t^{i,j}$ and the approximate likelihood $\tilde{u}_t^{i,j}$ from layer 3, and compute the non-normalized importance weight $\tilde{v}_t^i$ which is output to layer 1.

At steps 2 and 3 we generate the predictive ensemble for the slow states, $\bar{\boldsymbol{X}}_t^i$, and the observations, $\boldsymbol{Y}_t^i$, respectively. These ensembles are then used, when the new observation $\boldsymbol{y}_t$ is collected, to compute an updated ensemble $\boldsymbol{X}_t^i$ which yields non-weighted particle approximation of the distribution with pdf $p(\boldsymbol{x}_t|\boldsymbol{y}_{1:t}, \bar{\boldsymbol{\theta}}_t^i)$. The update step of the EnKF can be implemented in different ways. Here we follow the scheme in [19] which avoids the direct computation of the inverse of the covariance observation matrix $(d_y \times d_y)$, being better suited for high-dimensional systems.

Third layer. In Algorithm 6 we describe how to use an EKF to obtain Gaussian approximations $\mathcal{N}(\boldsymbol{z}_q|\check{\boldsymbol{z}}_q, \check{\boldsymbol{C}}_q(\boldsymbol{z})) \approx p(\boldsymbol{z}_q|\boldsymbol{x}_{t-1}^{i,j}, \boldsymbol{y}_{1:t-1}, \bar{\boldsymbol{\theta}}_t^i)$, $q = h(t-1)+1, \ldots, ht$, and the updated pdf $\mathcal{N}(\boldsymbol{z}_{ht}|\hat{\boldsymbol{z}}_{ht}^{i,j}, \hat{\boldsymbol{C}}_{ht}^{i,j}(\boldsymbol{z})) \approx p(\boldsymbol{z}_{ht}|\bar{\boldsymbol{x}}_t^{i,j}, \boldsymbol{x}_{t-1}^{i,j}, \boldsymbol{y}_{1:t}, \bar{\boldsymbol{\theta}}_t^i)$. We also generate the new slow states at time t, denoted $\bar{\boldsymbol{x}}_t^{i,j}$, and the likelihood estimates $\tilde{u}_t^{i,j} \approx p(\boldsymbol{y}_t|\bar{\boldsymbol{x}}_t^{i,j}, \boldsymbol{x}_{0:t-1}^{i,j}, \boldsymbol{y}_{1:t-1}, \bar{\boldsymbol{\theta}}_t^i)$. Note that all computations in this layer are conditional on $\boldsymbol{x}_{t-1}^{i,j}$ and $\bar{\boldsymbol{\theta}}_t^i$.

In step 1, the algorithm propagates the mean, $\hat{\boldsymbol{z}}_{h(t-1)}^{i,j}$, and the covariance matrix, $\hat{\boldsymbol{C}}_{h(t-1)}^{i,j}(\boldsymbol{z})$, for $q = h(t-1)+1, \ldots, ht$, conditional on the parameters $\bar{\boldsymbol{\theta}}_t^i$ and slow variables $\boldsymbol{x}_{t-1}^{i,j}$. At each time step q, we obtain a predictive mean, $\check{\boldsymbol{z}}_q^{i,j}$, and the predictive covariance matrix, $\check{\boldsymbol{C}}_q^{i,j}(\boldsymbol{z})$. The average of the predictive means, $\bar{\boldsymbol{z}}_t^{i,j} = \frac{1}{h}\sum_{q=h(t-1)+1}^{ht} \check{\boldsymbol{z}}_q^{i,j}$, is then used to propagate the slow state $\boldsymbol{x}_{t-1}^{i,j}$

and generate the new sample $\bar{\boldsymbol{x}}_t^{i,j}$ from the Gaussian approximation

$$\mathcal{N}(\boldsymbol{x}_t|\check{\boldsymbol{x}}_t^{i,j}, \Delta_x \boldsymbol{Q}_x) \approx p(\boldsymbol{x}_t|\boldsymbol{x}_{t-1}^{i,j}, \boldsymbol{y}_{1:t-1}, \bar{\boldsymbol{\theta}}_t^i)$$

at step 2. Note that the covariance of the $\boldsymbol{z}_q^{i,j}$'s is neglected for simplicity in this computation and we use just the covariance matrix $\Delta_x \boldsymbol{Q}_x$ of the slow state in Eq. (3).

In step 3 we project the predictive mean $\check{\boldsymbol{z}}_{ht}^{i,j}$ and the sample $\bar{\boldsymbol{x}}_t^{i,j}$ into the observation space to obtain the predictive observation $\hat{\boldsymbol{y}}_t^{i,j}$. When the *actual* observation $\boldsymbol{y}_t$ is available we also estimate the likelihood $p(\boldsymbol{y}_t|\bar{\boldsymbol{x}}_t^{i,j}, \boldsymbol{x}_{0:t-1}^{i,j}, \boldsymbol{y}_{1:t-1}, \bar{\boldsymbol{\theta}}_t^i)$ as

$$\tilde{u}_t^{i,j} = p(\boldsymbol{y}_t|\check{\boldsymbol{z}}_{ht}^{i,j}, \bar{\boldsymbol{x}}_t^{i,j}, \bar{\boldsymbol{\theta}}_t^i) p(\boldsymbol{x}_t|\check{\boldsymbol{z}}_{h(t-1)+1:ht}^{i,j}, \boldsymbol{x}_{t-1}^{i,j}, \bar{\boldsymbol{\theta}}_t^i).$$

Note that we use the predictive means $\check{\boldsymbol{z}}_{h(t-1):ht}^{i,j}$ for simplicity, instead of actually integrating w.r.t. the random states $\boldsymbol{z}_{h(t-1):ht}$.

Finally, in step 4, we compute the Kalman gain using the predictive covariance matrix of Eq. (50) and the Jacobian matrix $\boldsymbol{H}_t^{i,j}(\boldsymbol{z})$. Then, we update the mean, $\hat{\boldsymbol{z}}_{ht}^{i,j}$, and covariance matrix, $\hat{\boldsymbol{C}}_{ht}^{i,j}(\boldsymbol{z})$, of the fast variables for the next time step.

Algorithm 4. *SMC approximation of $p(\boldsymbol{\theta}|\boldsymbol{y}_{1:t})$ in the second method* **Inputs**

- *Prior distributions $p(\boldsymbol{\theta})$, $p(\boldsymbol{x}_0)$ and $p(\boldsymbol{z}_0)$.*

- *A Markov kernel $\kappa_N^{\boldsymbol{\theta}'}(d\boldsymbol{\theta})$ which, given $\boldsymbol{\theta}'$, generates jittered parameters $\boldsymbol{\theta} \in \mathbb{R}^{d_\theta}$.*

Initialization: *this is a joint initialization for all three layers.*

- *Draw N i.i.d. sample $\boldsymbol{\theta}_0^i$, $i = 1, \ldots, N$ from the prior distribution $p(\boldsymbol{\theta})$.*

- *Draw NJ i.i.d. samples $\boldsymbol{x}_0^{i,j}$, $i = 1, \ldots, N$, $j = 1, \ldots, J$, from the prior distribution $p(\boldsymbol{x}_0)$, and build the ensembles $\boldsymbol{X}_0^i$, $i = 1, \ldots, N$, as*

$$\boldsymbol{X}_0^i = [\boldsymbol{x}_0^{i,1}, \ldots, \boldsymbol{x}_0^{i,J}]. \tag{40}$$

- Set $\hat{\boldsymbol{z}}_0^{i,j} = \bar{\boldsymbol{z}}_0$ and $\hat{\boldsymbol{C}}_0^{i,j}(\boldsymbol{z}) = \boldsymbol{C}_0$, for $i = 1, \ldots, N$, $j = 1, \ldots, J$, where $\bar{\boldsymbol{z}}_0$ and $\boldsymbol{C}_0$ are the prior mean and prior covariance of $\boldsymbol{z}_0$, respectively, obtained from the prior density $p(\boldsymbol{z}_0)$.

Procedure *For $t \geq 0$:*

1. *Draw N i.i.d samples $\bar{\boldsymbol{\theta}}_t^i$ from $\kappa_N^{\boldsymbol{\theta}_{t-1}^i}(d\boldsymbol{\theta})$.*

2. *For $i = 1, \ldots, N$:*

   (a) *Retrieve*
   $$\tilde{v}_t^i = \hat{p}^J(\boldsymbol{y}_t | \boldsymbol{y}_{1:t-1}, \bar{\boldsymbol{\theta}}_t^i), \tag{41}$$
   where the approximate likelihood is evaluated at layer 2.

   (b) *Obtain new particles $\{\hat{\boldsymbol{X}}_t^i, \{\hat{\boldsymbol{z}}_{ht}^{i,j}, \hat{\boldsymbol{C}}_t^{i,j}(\boldsymbol{z})\}_{1 \leq j \leq J}\}$ at time t (from layers 2 and 3).*

   (c) *Normalize the weights*
   $$v_t^i = \frac{\tilde{v}_t^i}{\sum_{i=1}^N \tilde{v}_t^i}. \tag{42}$$

3. *Resample: set for each $m = 1, \ldots, N$*
   $$\{\boldsymbol{\theta}_t^m, \boldsymbol{X}_t^m, \{\hat{\boldsymbol{z}}_{ht}^{m,j}, \hat{\boldsymbol{C}}_t^{m,j}(\boldsymbol{z})\}_{j=1}^J\} = \{\bar{\boldsymbol{\theta}}_t^i, \hat{\boldsymbol{X}}_t^i, \{\hat{\boldsymbol{z}}_{ht}^{i,j}, \hat{\boldsymbol{C}}_t^{i,j}(\boldsymbol{z})\}_{j=1}^J\} \tag{43}$$
   with probability v_t^i.

Outputs: $\{\boldsymbol{\theta}_t^i, \boldsymbol{X}_t^i, \{\hat{\boldsymbol{z}}_{ht}^{i,j}, \hat{\boldsymbol{C}}_t^{i,j}(\boldsymbol{z})\}_{j=1}^J\}_{i=1}^N$.

Algorithm 5. *EnKF approximation of $p(\boldsymbol{x}_t | \boldsymbol{y}_{1:t}, \boldsymbol{\theta})$*

   Inputs

   - *Parameter vector $\bar{\boldsymbol{\theta}}_t^i$; ensemble of slow states, $\boldsymbol{X}_{t-1}^i = [\boldsymbol{x}_{t-1}^{i,1}, \ldots, \boldsymbol{x}_{t-1}^{i,J}]$; mean vector $\hat{\boldsymbol{z}}_{h(t-1)}^{i,j}$ and the covariance matrix $\hat{\boldsymbol{C}}_{t-1}^{i,j}(\boldsymbol{z})$, for $j = 1, \ldots, J$.*

Procedure For $t \geq 0$:

1. For $j = 1, \ldots, J$:

   (a) Retrieve the new sample $\bar{\boldsymbol{x}}_t^{i,j}$ and the likelihood estimate $\tilde{u}_t^{i,j}$ from layer 3 and compute the non-normalized importance weight

   $$\tilde{v}_t^i \;=\; \frac{1}{J} \sum_{j=1}^{J} \tilde{u}_t^{i,j}, \tag{44}$$

   (b) Obtain the new mean $\hat{\boldsymbol{z}}_{ht}^{i,j}$ and covariance matrix $\hat{\boldsymbol{C}}_t^{i,j}(\boldsymbol{z})$ at time t, from layer 3.

2. Compute the predictive mean $\check{\boldsymbol{x}}_t^i$ and construct the predictive ensemble $\bar{\boldsymbol{X}}_t^i$ as

   $$\check{\boldsymbol{x}}_t^i = \frac{1}{J} \sum_{j=1}^{J} \bar{\boldsymbol{x}}_t^{i,j} \quad and \quad \bar{\boldsymbol{X}}_t^i = [\bar{\boldsymbol{x}}_t^{i,1}, \ldots, \bar{\boldsymbol{x}}_t^{i,J}]. \tag{45}$$

3. Obtain predictive observations $\tilde{\boldsymbol{y}}_t^{i,j}$ from layer 3, then compute the mean $\hat{\boldsymbol{y}}_t^i$ and the ensemble $\boldsymbol{Y}_t^i$ as

   $$\hat{\boldsymbol{y}}_t^i \;=\; \frac{1}{J} \sum_{j=1}^{J} \tilde{\boldsymbol{y}}_t^{i,j} \quad and \quad \boldsymbol{Y}_t^i = [\tilde{\boldsymbol{y}}_t^{i,1}, \ldots, \tilde{\boldsymbol{y}}_t^{i,J}], \quad for \ j = 1, \ldots, J. \tag{46}$$

4. Update the ensemble of slow variables

   $$\boldsymbol{C}_t^i(\boldsymbol{x}, \boldsymbol{y}) \;=\; \frac{1}{J} \tilde{\boldsymbol{X}}_t^i (\tilde{\boldsymbol{Y}}_t^i)^\top,$$

   $$\left(\boldsymbol{C}_t^i(\boldsymbol{y})\right)^{-1} \;=\; \boldsymbol{R}^{-1} - \boldsymbol{R}^{-1} \frac{1}{J} \tilde{\boldsymbol{Y}}_t^i \left(\boldsymbol{I}_J + (\tilde{\boldsymbol{Y}}_t^i)^\top \boldsymbol{R}^{-1} \frac{1}{J} \tilde{\boldsymbol{Y}}_t^i\right)^{-1} (\tilde{\boldsymbol{Y}}_t^i)^\top \boldsymbol{R}^{-1},$$

   $$\boldsymbol{K}_t(\boldsymbol{x}) \;=\; \boldsymbol{C}_t^i(\boldsymbol{x}, \boldsymbol{y}) \left(\boldsymbol{C}_t^i(\boldsymbol{y})\right)^{-1}, \tag{47}$$

   $$\hat{\boldsymbol{X}}_t^i \;=\; \bar{\boldsymbol{X}}_t^i + \boldsymbol{K}_t(\boldsymbol{x}) \left(\boldsymbol{y}_t \mathbb{1}_{d_y \times J} + \boldsymbol{T}_t^i - \boldsymbol{Y}_t^i\right), \tag{48}$$

   where $\tilde{\boldsymbol{X}}_t^i = \bar{\boldsymbol{X}}_t^i - \check{\boldsymbol{x}}_t^i \mathbb{1}_{d_x \times J}$ and $\tilde{\boldsymbol{Y}}_t^i = \boldsymbol{Y}_t^i - \hat{\boldsymbol{y}}_t^i \mathbb{1}_{d_y \times J}$, $\boldsymbol{C}_t^i(\boldsymbol{x}, \boldsymbol{y})$ is the cross covariance matrix, $\boldsymbol{C}_t^i(\boldsymbol{y})$ is the covariance matrix of the observation, $\boldsymbol{R}$ is the covariance matrix of the noise in the observation equation, $\mathbb{1}_{a \times b}$ is a $a \times b$ matrix of ones and $\boldsymbol{T}_t^i = \left[\boldsymbol{r}_t^1, \ldots, \boldsymbol{r}_t^J\right]$ with $\boldsymbol{r}_t^j \sim \mathcal{N}(\boldsymbol{r}_t | \boldsymbol{0}, \boldsymbol{R})$ is a matrix of Gaussian perturbations.

Outputs: $\hat{\boldsymbol{X}}_t^i$, $\{\hat{\boldsymbol{z}}_{ht}^{i,j}, \hat{\boldsymbol{C}}_t^{i,j}(\boldsymbol{z})\}_{j=1}^J$ and $\tilde{v}_t^i$.

Algorithm 6. *EKF approximation of* $p(\boldsymbol{z}_{ht}|\boldsymbol{x}_t, \boldsymbol{y}_{1:t}, \boldsymbol{\theta})$

    Inputs

- *Integration steps* Δ_x, Δ_z *and time scale ratio* $h = \frac{\Delta_x}{\Delta_z} \in \mathbb{Z}^+$.

- *Parameter vector* $\bar{\boldsymbol{\theta}}_t^i$; *slow states* $\boldsymbol{x}_{t-1}^{i,j}$ *(i.e. the j-th column of* $\boldsymbol{X}_{t-1}^i$*) and mean fast state* $\hat{\boldsymbol{z}}_{h(t-1)}^{i,j}$ *with covariance matrix* $\hat{\boldsymbol{C}}_{t-1}^{i,j}(\boldsymbol{z})$.

    Procedure *For* $t \geq 0$:

1. *Set* $\check{\boldsymbol{z}}_{h(t-1)}^{i,j} = \boldsymbol{z}_{h(t-1)}^{i,j}$ *and* $\check{\boldsymbol{C}}_q^{i,j}(\boldsymbol{z}) = \boldsymbol{C}_{h(t-1)}^{i,j}(\boldsymbol{z})$.
   For $q = h(t-1)+1, ..., ht$, *compute*

$$\check{\boldsymbol{z}}_q^{i,j} = \check{\boldsymbol{z}}_{q-1}^{i,j} + \Delta_z(f_{\boldsymbol{z}}(\check{\boldsymbol{z}}_{q-1}^{i,j}, \bar{\boldsymbol{\theta}}_t^i) + g_{\boldsymbol{z}}(\boldsymbol{x}_{t-1}^{i,j}, \bar{\boldsymbol{\theta}}_t^i)), \qquad (49)$$

$$\check{\boldsymbol{C}}_q^{i,j}(\boldsymbol{z}) = \boldsymbol{J}_q^{i,j}(\boldsymbol{z})\check{\boldsymbol{C}}_{q-1}^{i,j}(\boldsymbol{z})\big(\boldsymbol{J}_q^{i,j}(\boldsymbol{z})\big)^\top + \Delta_z\boldsymbol{Q}_z, \qquad (50)$$

    where $\boldsymbol{J}_q^{i,j}(\boldsymbol{z})$ *is the Jacobian matrix of the transition function of* $\boldsymbol{z}$ *and* $\Delta_z\boldsymbol{Q}_z$ *is the covariance matrix of the noise in Eq. (4).*

2. *In the space of the slow state variables:*

   (a) *Project the predictive means* $\check{\boldsymbol{z}}_{h(t-1)+1:ht}^{i,j}$ *into the space of slow variables,*

$$\check{\boldsymbol{x}}_t^{i,j} = \boldsymbol{x}_{t-1}^{i,j} + \Delta_x(f_{\boldsymbol{x}}(\boldsymbol{x}_{t-1}^{i,j}, \bar{\boldsymbol{\theta}}_t^i) + g_{\boldsymbol{x}}(\bar{\boldsymbol{z}}_t^{i,j}, \bar{\boldsymbol{\theta}}_t^i)), \qquad (51)$$

    where $\bar{\boldsymbol{z}}_t^{i,j} = \frac{1}{h}\sum_{q=h(t-1)+1}^{ht} \check{\boldsymbol{z}}_q^{i,j}$.

   (b) *Sample* $\bar{\boldsymbol{x}}_t^{i,j} \sim \mathcal{N}(\boldsymbol{x}_t|\check{\boldsymbol{x}}_t^{i,j}, \Delta_x\boldsymbol{Q}_x)$, *where* $\Delta_x\boldsymbol{Q}_x$ *is the covariance matrix of the noise in Eq. (3).*

3. *When a new observation* $\boldsymbol{y}_t$ *is collected:*

28

(a) *Project the predictive mean $\check{z}_{ht}^{i,j}$ and the slow state $\bar{x}_t^{i,j}$ into the observation space*

$$\tilde{y}_t^{i,j} = l(\check{z}_{ht}^{i,j}, \bar{x}_t^{i,j}, \bar{\theta}_t^i). \tag{52}$$

(b) *Compute $\tilde{u}_t^{i,j} = p(y_t|\check{z}_{ht}^{i,j}, \bar{x}_t^{i,j}, \bar{\theta}_t^i)p(x_t|\check{z}_{h(t-1)+1:ht}^{i,j}, x_{t-1}^{i,j}, \bar{\theta}_t^i)$. This is an estimate of the likelihood $p(y_t|\bar{x}_t^{i,j}, x_{0:t-1}^{i,j}, y_{1:t-1}, \bar{\theta}_t^i)$.*

4. *Update the mean and the covariance matrix of the fast variables*

$$K_t(z) = \check{C}_{ht}^{i,j}(z)H_t^{i,j}(z)^\top \left(H_t^{i,j}(z)\check{C}_{ht}^{i,j}(z)H_t^{i,j}(z)^\top + R \right)^{-1}, \tag{53}$$

$$\hat{z}_{ht}^{i,j} = \check{z}_{ht}^{i,j} + K_t(z)\left(y_t - \tilde{y}_t^{i,j}\right) \quad and \tag{54}$$

$$\hat{C}_{ht}^{i,j}(z) = \left(I_{d_z} - K_t(z)H_t^{i,j}(z) \right)\check{C}_{ht}^{i,j}(z), \tag{55}$$

where $H_t^{i,j}(z)$ is the Jacobian matrix of function $l(\cdot, \bar{x}_t^{i,j}, \bar{\theta}_t^i)$ w.r.t. $\check{z}_{ht}^{i,j}$ and R is the covariance matrix of the noise in the observation equation. We obtain the approximation $\mathcal{N}(z_{ht}|\hat{z}_{ht}^{i,j}, \hat{C}_{ht}^{i,j}(z)) \approx p(z_{ht}|\bar{x}_t^{i,j}, x_{0:t-1}^{i,j}, y_{0:t}, \bar{\theta}_t^i)$.

Outputs: $\hat{z}_{ht}^{i,j}, \hat{C}_{ht}^{i,j}(z)$, $\bar{x}_t^{i,j}$ and $\tilde{u}_t^{i,j}$.

---

5. Example

5.1. Stochastic two-scale Lorenz 96 model

In order to illustrate the application of the methods described in Section 4, we consider a stochastic version of the two-scale Lorenz 96 model [4], which depends on a set of fixed parameters, a set of fast variables and a set of slow variables. The slow variables are represented by a d_x-dimensional vector, x, while the fast variables, z, are d_z-dimensional. Let us assume there are R fast variables per slow variable, therefore $d_z = Rd_x$. The system is described, in continuous-time τ, by the SDEs

$$dx_j = \left[-x_{j-1}(x_{j-2} - x_{j+1}) - x_j + F - \frac{HC}{B}\sum_{l=(j-1)R}^{Rj-1} z_l \right]d\tau + \sigma_x dv_j, \tag{56}$$

$$dz_l = \left[-CBz_{l+1}(z_{l+2} - z_{l-1}) - Cz_l + \frac{CF}{B} + \frac{HC}{B}x_{\lfloor (l-1)/R \rfloor} \right]d\tau + \sigma_z dw_l \tag{57}$$

where $j = 0, \ldots, d_x - 1$, $l = 0, \ldots, d_z - 1$; $\boldsymbol{v} = (v_0, \ldots, v_{d_x-1})^\top$ and $\boldsymbol{w} = (w_0, \ldots, w_{d_z-1})^\top$ are, respectively, d_x- and d_z-dimensional vectors of independent standard Wiener processes; $\sigma_x > 0$ and $\sigma_z > 0$ are known scale parameters and $\boldsymbol{\theta} = (F, H, C, B)^\top \in \mathbb{R}$ are static model parameters. Using a micro-macro solver [31, 35] that runs an Euler-Maruyama scheme at each time-scale to integrate Eqs. (56)–(57), the discrete-time state equation can be written as

$$
\begin{aligned}
x_{t+1,j} &= x_{t,j} + \Delta_x (f_{\boldsymbol{x},j}(\boldsymbol{x}_t, \boldsymbol{\theta}) + g_{\boldsymbol{x},j}(\bar{\boldsymbol{z}}_{t+1}, \boldsymbol{\theta})) + \sqrt{\Delta_x} \sigma_x v_{t+1,j}, \quad (58) \\
z_{n+1,l} &= z_{n,l} + \Delta_z (f_{\boldsymbol{z},l}(\boldsymbol{x}_{\lfloor \frac{n}{h} \rfloor}, \boldsymbol{\theta}) + g_{\boldsymbol{z},l}(\boldsymbol{z}_n, \boldsymbol{\theta})) + \sqrt{\Delta_z} \sigma_z w_{n+1,l}, \quad (59)
\end{aligned}
$$

where

$$
\boldsymbol{x}_t = (x_{t,0}, \ldots, x_{t,d_x-1})^\top \quad \text{and} \quad \boldsymbol{z}_n = (z_{n,0}, \ldots, z_{n,d_z-1})^\top
$$

are the discrete-time slow and fast variables, respectively; $\bar{\boldsymbol{z}}_t$ is the time-average

$$
\bar{\boldsymbol{z}}_t = \frac{1}{h} \sum_{n=h(t-1)+1}^{ht} \boldsymbol{z}_n
$$

and we denote $\bar{\boldsymbol{z}}_t = (\bar{z}_{t,0}, \ldots, \bar{z}_{t,d_z-1})^\top$; the terms $v_{t,j}$ and $w_{n,l}$ are independent Gaussian variables with identical $\mathcal{N}(\cdot|0,1)$ pdf for all t, j, n and l, and the functions

$$
\begin{aligned}
f_{\boldsymbol{x},j} &: \quad \mathbb{R}^{d_x} \times \mathbb{R}^{d_\theta} \to \mathbb{R}^{d_x}, \\
g_{\boldsymbol{x},j} &: \quad \mathbb{R}^{d_z} \times \mathbb{R}^{d_\theta} \to \mathbb{R}^{d_x}, \\
f_{\boldsymbol{z},l} &: \quad \mathbb{R}^{d_x} \times \mathbb{R}^{d_\theta} \to \mathbb{R}^{d_z} \quad \text{and} \\
g_{\boldsymbol{z},l} &: \quad \mathbb{R}^{d_z} \times \mathbb{R}^{d_\theta} \to \mathbb{R}^{d_z}
\end{aligned}
$$

can be expressed as

$$
\begin{aligned}
f_{\boldsymbol{x},j}(\boldsymbol{x}_t, \boldsymbol{\theta}) &= -x_{t,j-1}(x_{t,j-2} - x_{t,j+1}) - x_{t,j} + F, \\
g_{\boldsymbol{x},j}(\bar{\boldsymbol{z}}_t, \boldsymbol{\theta}) &= -\frac{HC}{B} \sum_{l=(j-1)R}^{Rj-1} \bar{z}_{t,l}, \\
f_{\boldsymbol{z},l}(\boldsymbol{x}_t, \boldsymbol{\theta}) &= \frac{HC}{B} x_{t,\lfloor (l-1)/R \rfloor} \quad \text{and} \\
g_{\boldsymbol{z},l}(\boldsymbol{z}_n, \boldsymbol{\theta}) &= -CB z_{n,l+1}(z_{n,l+2} - z_{n,l-1}) - C z_{n,l} + \frac{CF}{B}.
\end{aligned}
$$

We assume that the observations are linear and Gaussian, namely,

$$\boldsymbol{y}_t = \boldsymbol{A}_t \begin{bmatrix} \boldsymbol{x}_t \\ \boldsymbol{z}_{ht} \end{bmatrix} + \boldsymbol{r}_t, \tag{60}$$

where $\boldsymbol{A}_t$ is a known $d_y \times (d_x + d_z)$ matrix and $\boldsymbol{r}_t$ is a d_y-dimensional Gaussian random vector with known covariance matrix

$$\boldsymbol{R} = \begin{bmatrix} \sigma_{y,x}^2 \boldsymbol{I}_{d_x} & \boldsymbol{0} \\ \boldsymbol{0} & \sigma_{y,z}^2 \boldsymbol{I}_{d_z} \end{bmatrix}, \tag{61}$$

and $\sigma_{y,x}^2, \sigma_{y,z}^2 > 0$ are known variances.

5.2. Numerical results

We have run simulations for the two-scale Lorenz 96 model of Section 5.1, with dimensions $d_x = 10$ and $d_z = 50$. The time steps for the Euler-Maruyama integrators are $\Delta_x = 10^{-3}$ and $\Delta_z = 10^{-4}$ continuous-time units. We set the fixed parameters as $F = 8$, $H = 0.75$, $C = 10$ and $B = 15$. In order to obtain the initial states $\boldsymbol{x}_0$ and $\boldsymbol{z}_0$, we simulate a deterministic version of Eqs. (58)–(59) ($\sigma_x = \sigma_z = 0$) for 20 continuous-time units. We set the initial states as the values of variables $\boldsymbol{x}$ and $\boldsymbol{z}$ at the last time step of this simulation. This initialization is used in all simulations of this computer experiment in order to generate both "ground truth" sequences of $\boldsymbol{x}_t$ and $\boldsymbol{z}_n$ and the associated sequences of observations $\boldsymbol{y}_t$. We set the matrix $\boldsymbol{A}_t = \boldsymbol{I}_{d_y}$, for $d_y = d_x + d_z$.

In the experiments, we compare the performance of both methods proposed (the first one of Section 4.1 and the second one of Section 4.2). We experiment with different number of samples N and J in the first and second layers of the former methods. Additionally, for the first method (SMC-SMC-UKF) we run the multi-scale hybrid filter with $L = 2d_z + 1 = 101$ sigma-points for the UKF in the third layer. We need to estimate $\boldsymbol{\theta} = [F, C, H, B]^\top$ (hence, $d_\theta = 4$). The prior for the unknown parameters is uniform, namely $p(\boldsymbol{\theta}) = \mathcal{U}([2, 20]^2)$, while the priors used in the filtering algorithm for both unknown state variables are Gaussian, namely $p(\boldsymbol{x}_0) = \mathcal{N}(\boldsymbol{x}_0, 0.1\boldsymbol{I}_{d_x})$ and $p(\boldsymbol{z}_0) = \mathcal{N}(\boldsymbol{z}_0, 10\boldsymbol{I}_{d_z})$. The noise scaling factors, $\sigma_x = \frac{1}{2}$, $\sigma_z = \frac{1}{16}$, $\sigma_{y,x} = 10^{-1}$ and $\sigma_{y,z} = 10^{-3}$, are known.

The jittering kernel is $\kappa_N^{\boldsymbol{\theta}'}(d\boldsymbol{\theta}) = \mathcal{N}(\boldsymbol{\theta}|\boldsymbol{\theta}', \tilde{\sigma}^2 \boldsymbol{I}_{d_\theta})$, where $\tilde{\sigma}^2 = \frac{0.05}{\sqrt{N^3}}$ is selected following [8].

We assess the accuracy of the algorithms in terms of the normalized mean square error (NMSE) of the estimators of the parameters, the slow state variables and the fast state variables. In the plots, we show the NMSEs computed at time t,

$$\text{NMSE}_{\boldsymbol{\theta},t} = \frac{\|\boldsymbol{\theta}_t - \hat{\boldsymbol{\theta}}_t\|^2}{\|\boldsymbol{\theta}_t\|^2}, \tag{62}$$

$$\text{NMSE}_{\boldsymbol{x},t} = \frac{\|\boldsymbol{x}_t - \hat{\boldsymbol{x}}_t\|^2}{\|\boldsymbol{x}_t\|^2}, \tag{63}$$

$$\text{NMSE}_{\boldsymbol{z},t} = \frac{\|\boldsymbol{z}_{ht} - \hat{\boldsymbol{z}}_{ht}\|^2}{\|\boldsymbol{z}_{ht}\|^2}, \tag{64}$$

averaged over 50 independent simulation runs of 20 continuous-time units each, where the estimators take the form

$$\hat{\boldsymbol{\theta}}_t = \sum_{i=1}^{N} v_t^i \boldsymbol{\theta}^i, \tag{65}$$

$$\hat{\boldsymbol{x}}_t = \sum_{i=1}^{N} \sum_{j=1}^{J} v_t^i u_t^{i,j} \boldsymbol{x}_t^{i,j} \quad \text{and} \tag{66}$$

$$\hat{\boldsymbol{z}}_{ht} = \sum_{i=1}^{N} \sum_{j=1}^{J} \sum_{l=0}^{L} v_t^i u_t^{i,j} \lambda_{ht}^{i,j,l} \boldsymbol{z}_{ht}^{i,j,l}, \tag{67}$$

for the first method. For the second method the estimators of the state variables are

$$\hat{\boldsymbol{x}}_t = \frac{1}{J} \sum_{i=1}^{N} \sum_{j=1}^{J} v_t^i \boldsymbol{x}_t^{i,j} \quad \text{and} \tag{68}$$

$$\hat{\boldsymbol{z}}_{ht} = \frac{1}{J} \sum_{i=1}^{N} \sum_{j=1}^{J} v_t^i \boldsymbol{z}_{ht}^{i,j}, \tag{69}$$

where $\boldsymbol{x}_t^{i,j}$ is the j-th member of the ensemble $\boldsymbol{X}_t^i$ in Algorithm 5.

Figure 2 shows the performance of the proposed methods for different values of J (number of samples in the second layer) and $N = 20$. This is evaluated in terms of averaged $\text{NMSE}_{\boldsymbol{\theta}}$, $\text{NMSE}_{\boldsymbol{x}}$ and $\text{NMSE}_{\boldsymbol{z}}$ together with the running time in hours. The first method (SMC-SMC-UKF) shows an improvement in the

accuracy as the number of samples J increases, although this improvement is only significant for the slow state (Fig. 2b). The second method (SMC-EnKF-EKF) remains stable with J. The second method outperforms the first one in accuracy of the parameter estimation (Fig. 2a) as well as the slow state estimation (Fig. 2b). However, the first method obtains a better $\text{NMSE}_{\boldsymbol{z}}$. Additionally, the second method runs faster since the computational cost is considerably lower.
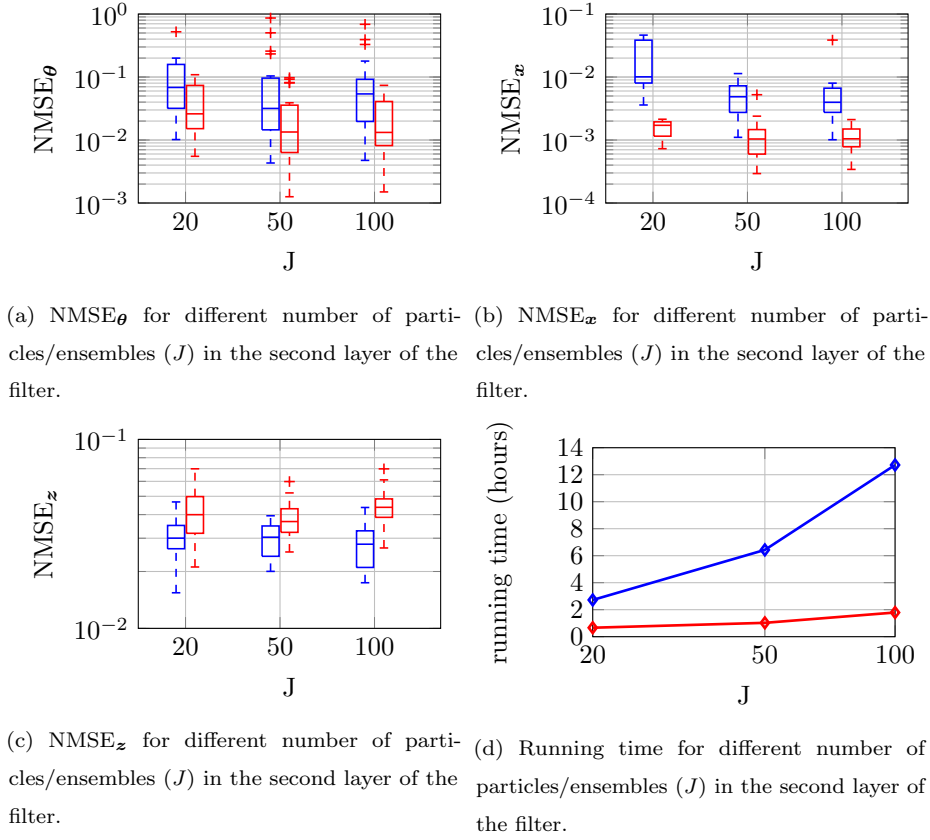

(a) $\text{NMSE}_{\boldsymbol{\theta}}$ for different number of particles/ensembles (J) in the second layer of the filter.

(b) $\text{NMSE}_{\boldsymbol{x}}$ for different number of particles/ensembles (J) in the second layer of the filter.

(c) $\text{NMSE}_{\boldsymbol{z}}$ for different number of particles/ensembles (J) in the second layer of the filter.

(d) Running time for different number of particles/ensembles (J) in the second layer of the filter.

Figure 2: Averaged $\text{NMSE}_{\boldsymbol{\theta}}$ (2a), $\text{NMSE}_{\boldsymbol{x}}$ (2b), $\text{NMSE}_{\boldsymbol{z}}$ (2c) and average running time (2d) of SMC-SMC-UKF (in blue) and SMC-EnKF-EKF (in red), averaged over 50 simulation runs. The number of particles of the first layer (SMC) is set to $N = 20$.

Figure 3 compares the performance of the proposed methods and the EnKF for different values of N (number of samples in the first layer) and $J = 50$.

This is shown with the averaged NMSE$_{\boldsymbol{\theta}}$, NMSE$_{\boldsymbol{x}}$ and NMSE$_{\boldsymbol{z}}$ together with the running time in hours. Similar to the previous figure, the first method (SMC-SMC-UKF) shows a slight improvement in the accuracy of the slow state estimation as the number of samples J increases (Fig. 3b). The second method (SMC-EnKF-EKF) remains stable with N. The second method outperforms the first one in accuracy of the parameter estimation (Fig. 3a) and the slow state estimation (Fig. 3b), but not for the fast state estimation (Fig. 3c). Again, the second method runs faster since the computational cost is considerably lower.
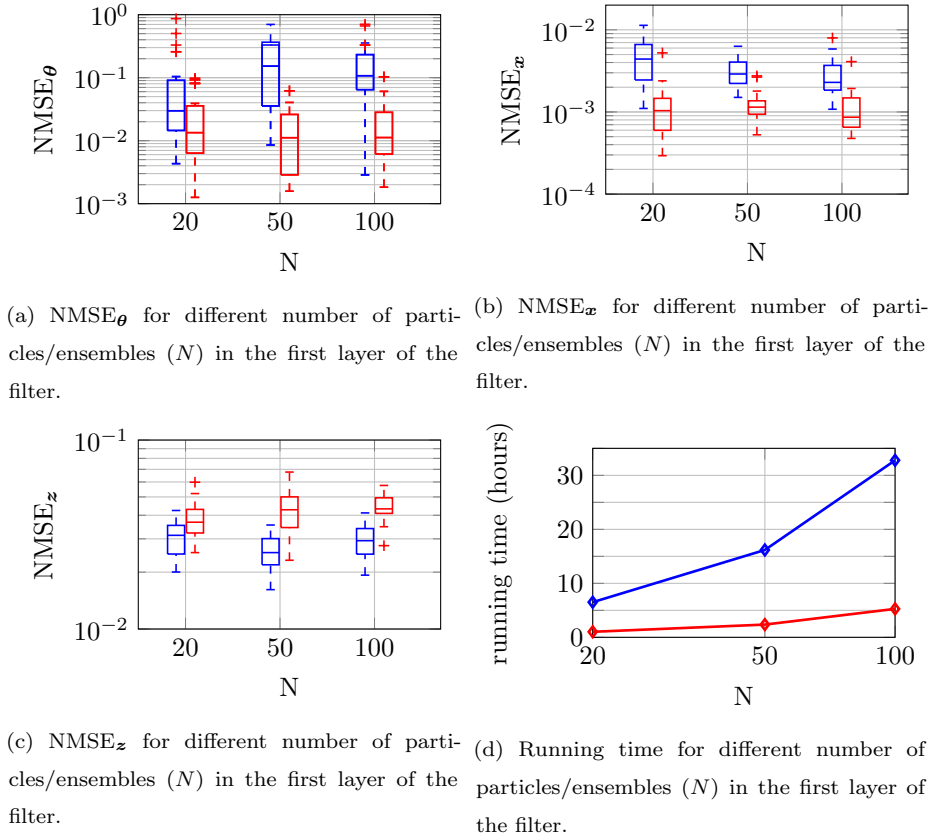

(a) NMSE$_{\boldsymbol{\theta}}$ for different number of particles/ensembles (N) in the first layer of the filter.

(b) NMSE$_{\boldsymbol{x}}$ for different number of particles/ensembles (N) in the first layer of the filter.

(c) NMSE$_{\boldsymbol{z}}$ for different number of particles/ensembles (N) in the first layer of the filter.

(d) Running time for different number of particles/ensembles (N) in the first layer of the filter.

Figure 3: Averaged NMSE$_{\boldsymbol{\theta}}$ (2a), NMSE$_{\boldsymbol{x}}$ (2b), NMSE$_{\boldsymbol{z}}$ (2c) and average running time (2d) of SMC-SMC-UKF (in blue) and SMC-EnKF-EKF (in red), averaged over 50 simulation runs. The number of particles/ensembles of the second layer (SMC for the first method and EnKF for the second method) is set to $J = 50$.

Finally, we show results for a computer experiment in which we have used the SMC-EnKF-EKF method to estimate the parameters F, C, B and H and track the state variables of the two-scale Lorenz 96 system with dimension $d_x = 10$ and $d_z = 50$. The number of particles used to approximate the sequence of parameter posterior distributions is $N = 50$ and the number of samples in the ensembles of the second layer is $J = 50$.

Figure 4 shows the true state trajectories, together with their estimates, for the first slow state variable (x_1) and the first fast state variable (z_1) of the two-scale Lorenz 96 model. We note that although the accuracy of the estimation of the fast variable is similar throughout the whole simulation run (over 20 continuous-time units), we only show the last 2 continuous-time units of the simulation.
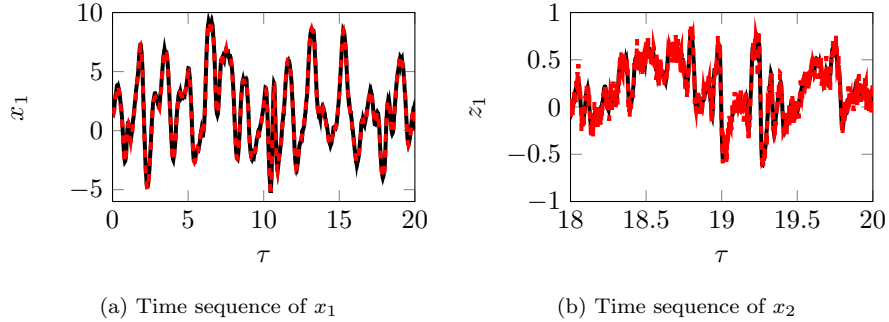

(a) Time sequence of x_1 (b) Time sequence of x_2

Figure 4: Sequences of state values (black line) and estimates (dashed red line) in x_1 (plot 4a) and z_1 (plot 4b) over time.

In Fig. 5 we observe the estimated posterior pdfs of the fixed parameters F, C, B and H, together with the ground truth values. Figure 5a displays the approximate posterior pdf of the parameter F (red dashed line) together with the true value $F = 8$ (vertical black line), Fig. 5b displays the approximate posterior pdf of the parameter C (blue dashed line) together with the true value $C = 10$ (vertical black line), Fig. 5c displays the approximate posterior pdf of the parameter B (green dashed line) together with the true value $B = 15$ (vertical black line) and Fig. 5d displays the approximate posterior pdf of the parameter

H (magenta dashed line) together with the true value $H = 0.75$ (vertical black line). We observe that for all the pdfs, nearly all probability mass is allocated close to the true values, except for the parameter B (Fig. 5c). In this case, the pdf is slightly shifted w.r.t. the true value.
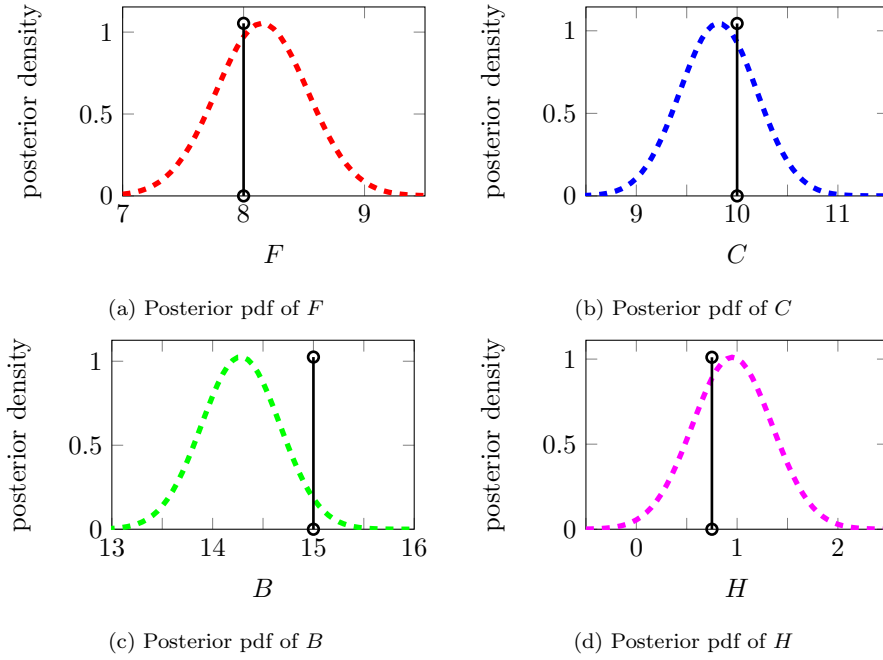

(a) Posterior pdf of F

(b) Posterior pdf of C

(c) Posterior pdf of B

(d) Posterior pdf of H

Figure 5: Posterior density of the parameters (dashed lines) at time $\tau = 20$. The true values are indicated by a black vertical line.

6. Conclusions

We have introduced a further generalization of the NHF methodology of [26] that, using long sequences of observations collected over time, estimates the static parameters and the stochastic dynamical variables of a class of heterogeneous multi-scale state-space models [1]. This scheme combines three layers of filters, one inside the other. It approximates recursively the posterior probability

distributions of the parameters and the two sets of state variables given the sequence of available observations. In a first layer of computation we approximate the posterior probability distribution of the parameters, in a second layer we approximate the posterior probability distribution of the slow state variables, and the posterior probability distribution of the fast state variables is approximated in a third layer. The inference techniques used in each layer can vary, leading to different computational costs and degrees of accuracy. To be specific, we describe two possible algorithms that derive from this scheme, combining Monte Carlo methods and Gaussian filters at different layers. The first method involves using sequential Monte Carlo (SMC) methods in both first and second layers, together with a bank of unscented Kalman filter (UKFs) in the third layer (i.e., the SMC-SMC-UKF). The second method employs a SMC in the first layer, ensemble Kalman filters (EnKFs) at the second layer and introduces the use of a bank of extended Kalman filters (EKFs) in the third layer (i.e., the SMC-EnKF-EKF). We have presented numerical results for a two-scale stochastic Lorenz 96 model with synthetic data and we have evaluated the performance of the algorithm in terms of the normalized mean square errors (NMSEs) for the parameters and the dynamic (slow and fast) state variables. The proposed implementations (both of them) obtain good results in terms of accuracy, having a considerably reduction in running time (i.e., the computational cost) with the second method. Further research is still needed, studying the stability of the multi-layer structure when the sequence of observations are rare and/or few. Moreover, we can compare the proposed algorithms with other methods, using the Lorenz 96 system but also other models.

Acknowledgements

References

[1] Assyr Abdulle, E Weinan, Björn Engquist, and Eric Vanden-Eijnden. The heterogeneous multiscale method. Acta Numerica, 21:1–87, 2012.

[2] B. D. O. Anderson and J. B. Moore. Optimal Filtering. Englewood Cliffs, 1979.

[3] C. Andrieu, A. Doucet, and R. Holenstein. Particle Markov chain Monte Carlo methods. Journal of the Royal Statistical Society B, 72:269–342, 2010.

[4] H. M. Arnold. Stochastic parametrisation and model uncertainty. PhD thesis, University of Oxford, 2013.

[5] Alexandros Beskos, Dan Crisan, Ajay Jasra, Kengo Kamatani, and Yan Zhou. A stable particle filter for a class of high-dimensional state-space models. Advances in Applied Probability, 49(1):24–48, 2017.

[6] Mallory Carlu, Francesco Ginelli, Valerio Lucarini, and Antonio Politi. Lyapunov analysis of multiscale dynamics: The slow manifold of the two-scale lorenz'96 model. arXiv preprint arXiv:1809.05065, 2018.

[7] Nicolas Chopin, Pierre E Jacob, and Omiros Papaspiliopoulos. SMC^2: an efficient algorithm for sequential analysis of state space models. Journal of the Royal Statistical Society: Series B (Statistical Methodology), 75(3):397–426, 2013.

[8] Dan Crisan, Joaquin Miguez, et al. Nested particle filters for online parameter estimation in discrete-time state-space Markov models. Bernoulli, 24(4A):3039–3086, 2018.

[9] P. M. Djurić, J. H. Kotecha, J. Zhang, Y. Huang, T. Ghirmai, M. F. Bugallo, and J. Míguez. Particle filtering. IEEE Signal Processing Magazine, 20(5):19–38, September 2003.

[10] A. Doucet, S. Godsill, and C. Andrieu. On sequential Monte Carlo Sampling methods for Bayesian filtering. Statistics and Computing, 10(3):197–208, 2000.

[11] Arnaud Doucet and Adam M Johansen. A tutorial on particle filtering and smoothing: Fifteen years later. Handbook of nonlinear filtering, 12(656-704):3, 2009.

[12] G. Evensen. The ensemble Kalman filter: Theoretical formulation and practical implementation. Ocean dynamics, 53(4):343–367, 2003.

[13] Ian Grooms and Yoonsang Lee. A framework for variational data assimilation with superparameterization. Nonlinear Processes in Geophysics, 22(5):601–611, 2015.

[14] Ian Grooms and Gregor Robinson. A hybrid particle-ensemble Kalman filter for problems with medium nonlinearity. Plos one, 16(3):e0248266, 2021.

[15] S. J. Julier and J. Uhlmann. Unscented filtering and nonlinear estimation. Proceedings of the IEEE, 92(2):401–422, March 2004.

[16] Nishanth Lingala, N Sri Namachchivaya, Nicolas Perkowski, and Hoong C Yeong. Particle filtering in high-dimensional chaotic systems. Chaos: An Interdisciplinary Journal of Nonlinear Science, 22(4):047509, 2012.

[17] J. S. Liu and R. Chen. Sequential Monte Carlo methods for dynamic systems. Journal of the American Statistical Association, 93(443):1032–1044, September 1998.

[18] Edward N Lorenz. Predictability: A problem partly solved. In Proc. Seminar on predictability, volume 1, 1996.

[19] Jan Mandel. Efficient implementation of the ensemble Kalman filter. University of Colorado at Denver and Health Sciences Center, Center for Computational Mathematics, 2006.

[20] Henrique MT Menegaz, João Y Ishihara, Geovany A Borges, and Alessandro N Vargas. A systematization of the unscented Kalman filter theory. IEEE Transactions on automatic control, 60(10):2583–2598, 2015.

[21] J. Miguez, D. Crisan, and I. P. Mari no. Particle filtering for Bayesian parameter estimation in a high dimensional state space model. In Proceedings of the 23rd European Signal Processing Conference (EUSIPCO), September 2015.

[22] Christian A Naesseth, Fredrik Lindsten, and Thomas B Schön. High-dimensional filtering using nested sequential Monte Carlo. IEEE Transactions on Signal Processing, 67(16):4177–4188, 2019.

[23] Grigoris Pavliotis and Andrew Stuart. Multiscale methods: averaging and homogenization. Springer Science & Business Media, 2008.

[24] Manuel Pulido, Pierre Tandeo, Marc Bocquet, Alberto Carrassi, and Magdalena Lucini. Stochastic parameterization identification using ensemble Kalman filtering combined with maximum likelihood methods. Tellus A: Dynamic Meteorology and Oceanography, 70(1):1–17, 2018.

[25] J. Uhlmann S. J. Julier and H. F. Durrant-Whyte. A new method for the non linear transformation of means and covariances in filters and estimators. IEEE Transactions Automatic Control, 3:477–482, March 2000.

[26] J. Míguez S. Pérez-Vieites, I. P. Mariño. Probabilistic scheme for joint parameter estimation and state prediction in complex dynamical systems. Physical Review E, 98(6), 063305, 2017.

[27] Naratip Santitissadeekorn and Christopher Jones. Two-stage filtering for joint state-parameter estimation. Monthly Weather Review, 143(6):2028–2042, 2015.

[28] Zheqi Shen, Youmin Tang, Xiaojing Li, Yanqiu Gao, and Junde Li. On the localization in strongly coupled ensemble data assimilation using a two-scale

lorenz model. <u>Nonlinear Processes in Geophysics Discussions</u>, pages 1–24, 2018.

[29] Tadashi Tsuyuki. Data assimilation in a two-scale model with Kalman filters. <u>CAS/JSC WGNE Research Activities in Atmospheric and Oceanic Modelling</u>, pages 27–28, 2012.

[30] Eric Vanden-Eijnden. Heterogeneous multiscale methods: a review. <u>Communications in Computational Physics2 (3)</u>, pages 367–450, 2007.

[31] Eric Vanden-Eijnden et al. Fast communications: Numerical techniques for multi-scale dynamical systems with stochastic effects. <u>Communications in Mathematical Sciences</u>, 1(2):385–391, 2003.

[32] Gabriele Vissio and Valerio Lucarini. A proof of concept for scale-adaptive parametrizations: the case of the lorenz'96 model. <u>Quarterly Journal of the Royal Meteorological Society</u>, 144(710):63–75, 2018.

[33] E Weinan. <u>Principles of multiscale modeling</u>. Cambridge University Press, 2011.

[34] E Weinan and Bjorn Engquist. Multiscale modeling and computation. <u>Notices of the AMS</u>, 50(9):1062–1070, 2003.

[35] E Weinan, Di Liu, and Eric Vanden-Eijnden. Analysis of multiscale methods for stochastic differential equations. <u>Communications on Pure and Applied Mathematics</u>, 58(11):1544–1585, 2005.

[36] Hoong C Yeong, Ryne T Beeson, N Sri Namachchivaya, and Nicolas Perkowski. Particle filters with nudging in multiscale chaotic systems: with application to the lorenz'96 atmospheric model. <u>Journal of Nonlinear Science</u>, pages 1–34, 2020.